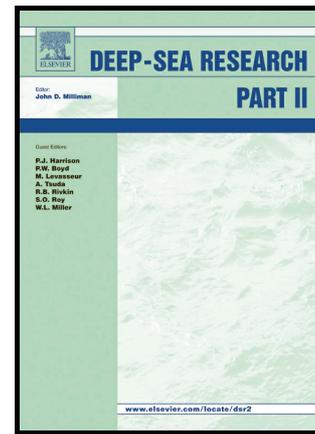# Author's Accepted Manuscript

Macronutrient supply, uptake and recycling in the coastal ocean of the west Antarctic Peninsula

Sian F. Henley, Robyn E. Tuerena, Amber L. Annett, Anthony E. Fallick, Michael P. Meredith, Hugh J. Venables, Andrew Clarke, Raja S. Ganeshram

Macronutrient supply, uptake and recycling in the coastal ocean of the west Antarctic Peninsula

Sian F. Henley[a*], Robyn E. Tuerena[a1], Amber L. Annett[a2], Anthony E. Fallick[b], Michael P. Meredith[c], Hugh J. Venables[c], Andrew Clarke[c], Raja S. Ganeshram[a]

[a]School of GeoSciences, University of Edinburgh, James Hutton Road, Edinburgh, EH9 3FE, UK
[b]Scottish Universities Environmental Research Centre, Rankine Avenue, East Kilbride, G75 0QF, UK
[c]British Antarctic Survey, High Cross, Madingley Road, Cambridge, CB3 0ET, UK

[*]Corresponding author: Sian F. Henley, email: s.f.henley@ed.ac.uk

Abstract

Nutrient supply, uptake and cycling underpin high primary productivity over the continental shelf of the west Antarctic Peninsula (WAP). Here we use a suite of biogeochemical and isotopic data collected over five years in northern Marguerite Bay to examine these macronutrient dynamics and their controlling biological and physical processes in the WAP coastal ocean.

We show pronounced nutrient drawdown over the summer months by primary production which drives a net seasonal nitrate uptake of 1.83 mol N m^{-2} yr^{-1}, equivalent to net carbon uptake of 146 g C m^{-2} yr^{-1}. High primary production fuelled primarily by deep-sourced macronutrients is diatom-dominated, but non-siliceous phytoplankton also play a role. Strong nutrient drawdown in the uppermost surface ocean has the potential to cause transient nitrogen limitation before nutrient resupply and/or regeneration. Interannual variability in nutrient utilisation corresponds to winter sea ice duration and the degree of upper ocean mixing, implying susceptibility to physical climate change.

The nitrogen isotope composition of nitrate ($\delta^{15}N_{NO3}$) shows a utilisation signal during the growing seasons with a community-level net isotope effect of 4.19 ± 0.29 ‰. We also observe significant deviation of our data from modelled and observed utilisation trends, and

[1] Present address: Department of Earth, Ocean and Ecological Sciences, University of Liverpool, Liverpool, L69 3GP, UK
[2] Present address: Department of Marine and Coastal Sciences, 71 Dudley Road, New Brunswick, NJ 08901-8525, USA

argue that this is driven primarily by water column nitrification and meltwater dilution of surface nitrate.

This study is important because it provides a detailed description of the nutrient biogeochemistry underlying high primary productivity at the WAP, and shows that surface ocean nutrient inventories in the Antarctic sea ice zone can be affected by intense recycling in the water column, meltwater dilution and sea ice processes, in addition to utilisation in the upper ocean.

Subject keywords: Nutrient cycles, nitrogen isotopes, primary production, phytoplankton, nutrient utilisation, Circumpolar Deep Water, nitrogen recycling, nitrification, sea ice, Regional index terms: Southern Ocean, Antarctic sea ice zone, west Antarctic Peninsula, Marguerite Bay, Ryder Bay

1. Introduction

1.1 Nutrients, primary production and CO_2 in the Southern Ocean

The Southern Ocean plays a crucial role in air-sea CO_2 exchange and consequently global climate over annual to glacial-interglacial timescales [*Caldeira and Duffy*, 2000; *Fletcher et al.*, 2006; *Gruber et al.*, 2009; *Lenton et al.*, 2013; *Sarmiento and LeQuere*, 1996; *Sigman and Boyle*, 2000]. The Antarctic continental shelves are particularly important for biological CO_2 uptake during photosynthesis by phytoplankton because area-normalised primary production rates here are greater than for any other Southern Ocean region [*Arrigo et al.*, 2008a]. As such, these shelf regions play a disproportionately strong role in the Southern Ocean carbon system and air-sea exchange of CO_2, such that changes here may have implications for large-scale biogeochemical cycles and climate [*Arrigo et al.*, 2008b].

The west Antarctic Peninsula (WAP) continental shelf is an ecologically-important region of high primary productivity, strong air-sea CO_2 fluxes and a large and productive food web [*Carrillo et al.*, 2004; *Clarke et al.*, 2008; *Ducklow et al.*, 2007; *Legge et al.*, 2015; *Montes-Hugo et al.*, 2010; *Ruiz-Halpern et al.*, 2014; *Schofield et al.*, 2010]. Primary production is regulated by the annual sea ice cycle, because the timing and distribution of phytoplankton blooms is modulated by ice extent and duration, coupled upper-ocean processes and their impact on light availability [*Smith and Comiso*, 2008; *Venables et al.*, 2013; *Vernet et al.*,

2008]. Primary production and biological CO_2 uptake are minimal during austral winter, due to extensive sea ice cover and low irradiance levels. As ice cover retreats in spring/early summer, large phytoplankton blooms can develop due to increased light availability, stratification of the upper water column by sea-ice meltwater and other freshwater inputs, and possible seeding of surface water blooms by sea-ice algae [*Clarke et al.*, 2008; *Smith and Nelson*, 1985]. In WAP coastal regions, summer chlorophyll levels often exceed 20 μg L^{-1} [*Ducklow et al.*, 2013; *Venables et al.*, 2013] and this high production and resultant uptake of CO_2 into organic matter is sufficient to create a seasonal biological sink for CO_2 [*Carrillo et al.*, 2004; *Legge et al.*, 2015; *Montes-Hugo et al.*, 2010; *Ruiz-Halpern et al.*, 2014]. Throughout autumn, primary production and biomass decrease to low winter levels due to shorter day-length, deepening of the mixed layer and decreasing phytoplankton growth rates, as well as high loss rates driven by zooplankton grazing, scavenging by sea ice, cell lysis and sedimentation [*Vernet et al.*, 2012]. Life cycles of the majority of Antarctic marine species and consequently the functioning of the entire marine ecosystem are paced by the annual advance and retreat of the ice pack, and its control of the key phytoplankton food source for higher organisms [*Clarke et al.*, 2008; *Ducklow et al.*, 2007]. Efficient carbon export (>10 % of net primary production) at the WAP also delivers a source of organic matter to subsurface and benthic food webs and may lead to longer-term CO_2 sequestration [*Buesseler et al.*, 2010; *Smith et al.*, 2012].

The supply and biogeochemical cycling of nutrients is critical for phytoplankton production, ecosystem function and their relationship to CO_2 dynamics [*Deutsch and Weber*, 2012]. In the Southern Ocean, and specifically over the WAP continental shelf, nutrients and CO_2 are supplied to the upper ocean via upwelling and mixing of Circumpolar Deep Waters (CDW) from the Antarctic Circumpolar Current (ACC) [*Carrillo et al.*, 2004; *Martinson et al.*, 2008; *Prezelin et al.*, 2000; *Serebrennikova and Fanning*, 2004]. Macronutrient supply from atmospheric, glacial or terrigenous inputs is thought to be negligible at the WAP, such that these deeper waters are the predominant nutrient source to phytoplankton blooms [*Dierssen et al.*, 2002; *Karl et al.*, 2002; *Pedulli et al.*, 2014]. These deep-sourced nutrients fuel primary production and biological uptake of CO_2, such that the large phytoplankton blooms observed at the WAP drive a substantial drawdown of macronutrients and CO_2 in surface waters over the summer months [*Clarke et al.*, 2008; *Ducklow et al.*, 2007]. The principal objective of this study is to provide a detailed description of the supply, uptake and cycling of macronutrients and their controlling biological and physical processes in northern Marguerite

Bay in the WAP coastal sea ice zone, based on a five-year high-resolution time-series of biogeochemical and isotopic data.

1.2 Nitrogen isotope systematics and tools

In addition to concentrations of nitrate, phosphate, silicic acid and ammonium, and the relationships between them, we also employ the nitrogen isotopic composition of nitrate ($\delta^{15}N_{NO3}$) as a useful tool for examination of nutrient biogeochemistry and marine nitrogen cycle processes. $\delta^{15}N$ is the per mille (‰) deviation of the $^{15}N/^{14}N$ ratio in the sample from the $^{15}N/^{14}N$ ratio in the universal reference standard atmospheric N_2, expressed as

$$\delta^{15}N \ (‰) = \left(\frac{(^{15}N/^{14}N) \ sample}{(^{15}N/^{14}N) \ standard} - 1 \right) x \ 1000 \qquad \text{Eq. 1}$$

Biological uptake of nitrate causes a kinetic fractionation between the ^{14}N and ^{15}N isotopes because phytoplankton preferentially assimilate the lighter energetically favoured ^{14}N isotope [*Sigman et al.*, 1999b and references therein]. As such, $\delta^{15}N_{NO3}$ increases as nitrate utilisation proceeds according to the fractionation factor or kinetic isotope effect (ϵ), which is defined by the ratio of the rates at which the two N isotopes are converted from nitrate to organic nitrogen:

$$\epsilon \ (‰) = (^{14}k/^{15}k - 1) \ x \ 1000 \qquad \text{Eq. 2}$$

^{14}k and ^{15}k are the rate coefficients of the reaction for ^{14}N- and ^{15}N-containing nitrate. Other nitrogen cycle processes, including organic matter remineralisation [*Saino and Hattori*, 1980, 1987], ammonium uptake [*Waser et al.*, 1998a; *Waser et al.*, 1998b], nitrification [*Casciotti et al.*, 2003; *Casbciotti*, 2009] and denitrification [*Granger et al.*, 2008 and references therein], also fractionate the ^{14}N and ^{15}N isotopes with characteristic isotope effects, such that $\delta^{15}N_{NO3}$ provides an integrative measure of all of the processes at work. $\delta^{15}N_{NO3}$ is used in this study to examine nutrient supply, uptake and recycling over the summer phytoplankton growing season in the high-productivity Antarctic coastal ocean.

1.3 Oceanographic and climatic context

The WAP is unusual in the Antarctic context, being one of only a few regions where the principal nutrient source water mass, CDW, intrudes onto the continental shelf in a much less modified form than in other Antarctic regions, and exerts a particularly direct influence on shelf ecosystems [*Hofmann et al.*, 1996]. The southern edge of the ACC lies adjacent to the

WAP shelf break such that CDW penetrates onto the shelf year-round, with the incursions being especially pronounced where glacially-scoured canyons dissect the shelf and reach to the shelf edge [*Dinniman and Klinck*, 2004; *Dinniman et al.*, 2011; *Martinson et al.*, 2008; *Martinson and McKee*, 2012; *Moffat et al.*, 2009]. Whilst lower circumpolar deep water (LCDW) is restricted to the deep canyons, upper circumpolar deep water (UCDW) bathes the WAP shelf up to shallow depths (below 200 m). Mixing and exchange of UCDW with overlying water masses as it moves across the shelf results in a modified form of this water mass in shelf environments, which is warm, saline and rich in nutrients and CO_2 compared with the overlying Antarctic Surface Water (AASW) [*Klinck*, 1998; *Montes-Hugo et al.*, 2010; *Prezelin et al.*, 2000; *Smith et al.*, 1999]. AASW is substantially fresher and less dense, creating a permanent pycnocline between 150 and 200 m [*Beardsley et al.*, 2004; *Hofmann and Klinck*, 1998; *Smith et al.*, 1999]. During the summer months, meltwater-induced freshening and solar warming of surface waters stratifies the upper ocean and leads to isolation of a remnant cold (<-1°C) layer of AASW, termed winter water (WW), centring on ~100 m depth between AASW and UCDW [*Mosby*, 1934]. Vertical mixing between UCDW, WW and AASW is driven by a range of processes including bathymetric interactions, internal tides, wind-induced shear, and coastal upwelling and downwelling, and permits the delivery of a substantial source of heat, salt, nutrients and CO_2 from UCDW to the productive surface ocean [*Howard et al.*, 2004; *Klinck et al.*, 2004; *Martinson*, 2012; *Montes-Hugo et al.*, 2010; *Prezelin et al.*, 2000; *Smith et al.*, 1999; *Wallace et al.*, 2008].

ACC waters advect northeastwards adjacent to the shelf slope, such that their incursion onto the shelf drives gyre-like surface water circulation over the shelf [*Klinck et al.*, 2004]. In the vicinity of Marguerite Bay and environs, the dominant current at depth is the flow of CDW along the glacially-scoured Marguerite Trough and into the bay itself [*Klinck et al.*, 2004]. Inshore, the seasonal buoyancy- and wind-forced Antarctic Peninsula coastal current (APCC) flows at shallow depths southwestwards along the coasts of Adelaide and Alexander Islands, with a presumed cyclonic circulation within Marguerite Bay [*Beardsley et al.*, 2004; *Moffat et al.*, 2008; *Savidge and Amft*, 2009]. Intermittent near-inertial currents have also been observed in Marguerite Bay during ice free periods [*Beardsley et al.*, 2004]. Whilst currents and flows at depth are crucial for the supply and distribution of UCDW over the shelf, surface water circulation pathways may be important for the transport of dissolved constituents such as nutrients, and plankton during the ice-free summer season.

In addition to its biogeochemical and ecological importance, the WAP has also experienced rapid and pronounced atmospheric and oceanic warming over the second half of the twentieth century [*Meredith and King*, 2005; *Vaughan et al.*, 2003]. Summer surface ocean temperatures over the WAP continental shelf have increased by more than 1˚C since the 1950s [*Meredith and King*, 2005] and deep temperatures are also warming [*Schmidtko et al.*, 2014]. These warming trends have been accompanied by a reduction in sea ice extent of 5.7 ± 1.0 % per decade [*Massom and Stammerjohn*, 2010], a shortening of the sea ice season by 3.3 months between 1979 and 2011 [*Stammerjohn et al.*, 2012], and widespread glacial retreat throughout the WAP region [*Cook et al.*, 2016]. Recent increases in the heat content and prevalence of UCDW across the WAP shelf have been identified as a crucial factor in driving these changes [*Martinson et al.*, 2008; *Martinson*, 2012; *Pritchard et al.*, 2012], and may influence the supply of macronutrients and CO_2 to shelf environments, with strong implications for air-sea gas exchange and climate feedbacks [*Montes-Hugo et al.*, 2010].

1.4 Objectives

Documented physical changes are already driving ecosystem changes at all levels of the food web [*Saba et al.*, 2014; *Schofield et al.*, 2010; *Venables et al.*, 2013] and concomitant biogeochemical change can be anticipated. This study aims to describe the supply, uptake and cycling of macronutrients over five years between 2004 and 2010 in the WAP coastal ocean. We examine variability in nutrient concentrations, ratios and isotopic signatures on seasonal, annual and interannual bases in order to elucidate the key biological and physical processes at work and their control of and by nutrient dynamics. This study will form the basis of a future research program to establish the ways in which nutrient biogeochemistry and the marine nitrogen cycle are changing in response to climate and oceanographic change in the WAP region.

2. Methods

2.1 Study location and field work

This study is set in Ryder Bay in northern Marguerite Bay at the WAP (Fig. 1), within the framework of the Rothera Time Series (RaTS) programme of the British Antarctic Survey, which has been running since 1997 [*Clarke et al.*, 2008; *Meredith et al.*, 2004; *Venables et al.*, 2013]. Seawater sampling and oceanographic monitoring were conducted approximately

twice-weekly during austral spring/summer growing seasons of 2004/05, 2005/06, 2006/07, 2008/09 and 2009/10, and approximately weekly during the intervening winter periods, as permitted by weather, ice and logistic constraints. Seawater samples were taken above the deepest point (~520 m) in Ryder Bay for determination of macronutrient concentrations and $\delta^{15}N_{NO3}$, alongside the routine samples for chlorophyll *a* concentration and oxygen isotope composition of seawater. Samples were taken from 15 m, the long-term average depth of the fluorescence maximum, in all years. Samples were also taken in depth profile over the surface mixed layer and from 100 m (the approximate core depth of WW) and 500 m (for UCDW) during summer 2009/10. Surface layer samples were taken using a 12 V electric bilge pump and acid-rinsed silicon tubing, transferred to acid-clean polyethylene containers and processed on return to the laboratory. All samples from 100 m and 500 m were collected using an acid-rinsed 5 L Niskin bottle and hand-operated winch.

2.2 Sample processing and analysis

2.2.1 Macronutrients

Samples for analysis of macronutrient (NO_3^-, NO_2^-, PO_4^{3-}) concentrations from 2009/10 were filtered through acid-rinsed 47 mm diameter 0.45 μm pore size HA nitrocellulose filters, frozen at -80˚C and subsequently stored at -20˚C until analysis. Analyses of $[NO_3^-+NO_2^-]$, $[NO_2^-]$ and $[PO_4^{3-}]$ were conducted using a Technicon AAII segmented flow autoanalysis system, from which raw data were corrected to elemental standards and ambient ocean salinity and pH [*Woodward and Rees*, 2001]. For simplicity, $[NO_3^-+NO_2^-]$ values are reported here as nitrate. Samples were assayed in duplicate or triplicate and standard deviation was generally better than 0.2 μmol L^{-1} for nitrate and 0.02 μmol L^{-1} for phosphate. Earlier in the time-series (2004-2009), macronutrient samples were filtered using GF/C filters and stored in dark polyethylene bottles in the dark at +4°C for up to one year, until analysis using standard autoanalyser protocols [*Clarke et al.*, 2008; *Strickland and Parsons*, 1968].

Samples for the determination of ammonium concentration were analysed within four hours of sample collection using ortho-phthaldialdehyde (OPA) and fluorometry [*Clarke et al.*, 2008; *Holmes et al.*, 1999]. Samples were assayed in triplicate, calibration is by standard addition at four concentrations, and the detection limit is 0.01 μmol L^{-1}.

Samples for analysis of dissolved silicic acid ($[Si(OH)_4^-]$) were filtered through acid-rinsed 47 mm diameter 0.6 µm pore size polycarbonate membrane filters, acidified with 1 ml L^{-1} of 50 % v/v HCl (Aristar grade) to prevent bacterial activity, and stored at room temperature [*Annett*, 2013]. Dissolved Si concentration was determined spectrophotometrically using HACH® reagents to produce a molybdenum-blue complex proportional to $[Si(OH)_4^-]$. Absorbance was measured at 812 nm with a spectrophotometer (1cm path length) and converted to $[Si(OH)_4^-]$ using a range of standard concentrations (0 – 90 µmol L^{-1}). Samples were analysed in duplicate or triplicate, and standard deviation was generally less than 1.0 µmol L^{-1}.

2.2.2 Nitrogen isotopic composition of nitrate

Samples were filtered through precombusted (450 ^{o}C for 4 hours) 25 mm diameter ~0.7 µm GF/F filters, and frozen until analysis. $\delta^{15}N_{NO3}$ was determined using the bacterial denitrifier method and isotope ratio mass spectrometry (IRMS) [*Sigman et al.*, 2001] at the Scottish Universities Environmental Research Centre (SUERC), East Kilbride, UK. Sample nitrate was converted to N_2O by denitrifying bacteria, *Pseudomonas aureofaciens*. N_2O was purified by chemical and cold traps on a custom-modified Analytical Precision gas-prep interface, a cryogenic focusing loop and gas chromatography, and analysed on a VG Prism III IRMS. Results are presented in the delta per mille notation relative to the international standard atmospheric N_2 ($\delta^{15}N$ ‰$_{AIR}$), after referencing raw data to atmospheric N_2 using isotopic standards USGS-32, USGS-34 and USGS-35 [*Böhlke et al.*, 2003]. Analytical precision (1σ) was around 0.2 ‰. All samples were analysed in duplicate and approximately half in triplicate; in each case, data were rejected where 1σ >0.5 ‰. Nitrite was not removed prior to denitrification, so the $\delta^{15}N_{NO3}$ values reported here are $\delta^{15}N$ of the combined nitrate+nitrite pool. The implications of this for our $\delta^{15}N_{NO3}$ data are discussed in section 4.1.

2.3 Oceanographic monitoring

Routine sea ice and oceanographic observations are taken in Ryder Bay [*Clarke et al.*, 2008]. Directly-observed daily sea ice concentrations compare well with satellite-derived regional ice cover of Marguerite Bay [*U.S. National Ice Center Products, NOAA,* 2012; available online at www.natice.noaa.gov/Main_Products.htm]. Water column profiling to 500 m depth was conducted concurrently with each water sampling event, with a SeaBird 19 Conductivity-Temperature-Depth (CTD) probe with a WetLabs in-line fluorometer and

LiCor photosynthetically active radiation (PAR) sensor. A range of parameters, including upper-ocean mixed layer depth (MLD), were derived from the CTD data.

3. Results and interpretation

3.1 Water column conditions and chlorophyll levels

Sea ice cover, MLD and chlorophyll data show a robust seasonal pattern (Fig. 2a) whereby winters are characterised by higher sea ice, deeper mixed layers and very low chlorophyll. Full fast-ice cover forms in most years, but the duration of cover shows large interannual variability. In spring and summer, sea ice retreats, the mixed layer shoals and chlorophyll reaches high levels of up to 25 µg L^{-1}. In autumn, the mixed layer deepens again, chlorophyll levels subside and sea ice cover increases. Significant interannual variability in MLD and chlorophyll, related to the duration of fast-ice cover, is superimposed onto this seasonality. During winters 2004, 2005 and 2006, winter fast-ice cover persisted for 4 – 7 months and MLD reached maxima of 67 m, 51 m and 46 m, respectively. Winters 2007 and 2008 were characterised by markedly lower sea ice with full cover lasting less than 1 month. Mixed layers were substantially deeper and more variable during these low-ice winters, with maxima of 167 m in 2007 and 118 m in 2008. Winter 2009 saw an intermediate two months of fast-ice cover and a somewhat shallower mixed layer than the two previous years, of maximum depth 102 m. Summer chlorophyll levels measured at 15 m also showed distinct interannual variability with concentrations >20 µg L^{-1} common in summers 2004/05, 2005/06 and 2006/07. In contrast, maximum chlorophyll was 7.7 and 5.4 µg L^{-1} in summers 2007/08 and 2008/09, respectively. Chlorophyll showed a small but significant recovery in 2009/10, consisting of a brief early-summer peak and a late-season bloom of up to 11.1 µg L^{-1} in February. Chlorophyll data are discussed in detail elsewhere [*Venables et al.*, 2013] and are only provided here as background for the biogeochemical investigations upon which our conclusions are based. Detailed biogeochemical data are not available for summer 2007/08, so this year is not discussed further.

Upper ocean salinity measured at 15 m also shows strong seasonality, being high during winter and decreasing over the course of summer to a minimum of 32.24 on the practical salinity scale (PSS) in February 2006 (Fig. 2b). The sea-ice meltwater fraction derived from the oxygen isotope composition of seawater [*Meredith et al.*, 2013] shows a seasonal pattern

in the earlier high-ice years (2004-2007) with minimum values during winter and increases over the summer seasons. This seasonal cycle breaks down in the later low-ice years, consistent with a shift to higher salinity overall and a less-pronounced seasonal cycle.

3.2 Seasonal variability in upper ocean macronutrient signatures

Macronutrient concentrations and $\delta^{15}N_{NO3}$ at 15 m also show characteristic seasonal cycles that are related to sea ice and chlorophyll dynamics (Fig. 2c-i). Although interannual variability is high, a robust seasonal cycle exists whereby concentrations of nitrate, phosphate and silicic acid are maximal during austral winter, decrease during the productive summer months, and recover through the autumn. Nitrate values typically range from 15 to 34 µmol L^{-1} in winter and decrease to summer minima of 0.13 to 8.2 µmol L^{-1}. Monthly-mean values calculated for all five seasons are around 20 µmol L^{-1} in winter and 9.2 µmol L^{-1} in the late summer. Phosphate values are 1.1 to 2.2 µmol L^{-1} during the winter and reach low summer values of 0.02 to 0.6 µmol L^{-1}. Monthly mean values are typically around 1.6 µmol L^{-1} in winter and 0.8 µmol L^{-1} in the late summer. A similar seasonal cycle exists for silicic acid, although variability is greater in general and the annual summer minimum appears to lag that of nitrate and phosphate by approximately one month. Monthly mean values are ~60 µmol L^{-1} in winter, reducing to 44 µmol L^{-1} in summer. Individual values can range from >80 µmol L^{-1} in winter to ≤30 µmol L^{-1} in summer. Ammonium follows a different seasonal cycle whereby concentrations are minimal in spring and early summer, increase through summer and into autumn, peak in autumn/early winter and then decline again back to the spring minimum. Spring values are mostly ≤0.7 µmol L^{-1} whilst winter values reach >3.5 µmol L^{-1} in each year. Monthly mean values are around 0.5 µmol L^{-1} at the spring minimum and up to 3 µmol L^{-1} at the early winter maximum. Nitrite concentration is generally <0.2 µmol L^{-1} during the summer seasons we studied, although occasional higher values up to 0.36 µmol L^{-1} are observed. Similar to ammonium, nitrite concentrations are minimal in spring and early summer, and maximal in winter.

The quasi-conservative tracer N* [*Gruber and Sarmiento*, 1997], modified here to incorporate the relatively high ammonium concentrations observed: N* = $[NO_3^- + NO_2^- + NH_4^+] - 16[PO_4^{3-}]$ (Fig. 2h), also shows a seasonal cycle that is related to addition and removal of dissolved inorganic nitrogen and phosphorus. N* values are minimal during winter (-8.33 ± 0.17 (1σ) µmol L^{-1}) and increase in spring and early summer to maximum

values during the summer phytoplankton bloom (2.18 ± 2.65 (1σ) μmol L^{-1}), before subsiding again into autumn.

$\delta^{15}N_{NO3}$ covaries with nitrate concentration in surface waters during the summer seasons (Fig. 2i). Prior to phytoplankton growth, high nitrate concentrations are accompanied by low $\delta^{15}N_{NO3}$ similar to the deep water nutrient source ($\sim$4.9 ‰, see below), due to vigorous vertical mixing over winter entraining deep waters into the upper ocean. As nitrate concentration decreases over the summer growing season, its isotopic composition becomes progressively enriched in ^{15}N, implicating fractionation by phytoplankton due to preferential uptake of the lighter ^{14}N isotope. At the greatest extent of nitrate drawdown ($[NO_3^-]$ <3 μmol L^{-1}), $\delta^{15}N_{NO3}$ reaches maximum values of >10 ‰. The relationship between $\delta^{15}N_{NO3}$ and nitrate concentration, and the derived parameter $\delta^{15}N_{nr}$ (Fig. 2j), are examined in detail in section 4.1.

As with any time-series location, some degree of the observed temporal variability could be the result of spatial heterogeneity in surface waters and lateral processes such as the movement of mesoscale eddies through the site. However, the length of the time-series and consistent seasonal patterns across all years strongly suggest that the observed seasonal cycles are robust and their magnitudes realistic, even if some small changes in nutrient concentrations and $\delta^{15}N_{NO3}$ arise from spatial variability.

3.3 Water column nutrient depth profiles

Depth profile data from summer 2009/10 show that macronutrient concentrations are highest at depth (200 to 500 m) and decrease into the surface layer, due to uptake by phytoplankton (Fig. 3). Temperature and salinity depth profiles are also shown to identify the key water masses; warm saline UCDW below $\sim$200 m, cold WW centring on $\sim$100 m, and AASW above, which warms and decreases in salinity over the course of the summer. Nitrate is 32.3 ± 1.2 μmol L^{-1} at 500 m and decreases to 13.9 ± 4.4 μmol L^{-1} at 15 m. As nitrate decreases into the upper ocean, its isotopic composition becomes progressively enriched in ^{15}N, such that $\delta^{15}N_{NO3}$ is 4.9 ± 0.4 ‰ at 500 m and increases to 7.4 ± 0.9 ‰ at 15 m. Phosphate concentration is 2.5 ± 0.2 μmol L^{-1} at 500 m and decreases to 1.2 ± 0.3 μmol L^{-1} at 15 m. Silicic acid concentration is 83.2 ± 4.4 μmol L^{-1} at 500 m and decreases to 45.4 ± 4.5 μmol L^{-1} at 15 m. During times of high production in the growing season, namely a short-lived phytoplankton bloom observed in early December and a larger phytoplankton bloom in February (Fig. 2a), there is a further drawdown of nitrate and phosphate above 15 m towards

the surface. For example, concentrations during the main phytoplankton bloom in February fall to $0.41 - 1.31$ µmol N L^{-1} and $0.30 - 0.38$ µmol P L^{-1} at 5 m, and $0.32 - 0.66$ µmol N L^{-1} and $0.27 - 0.31$ µmol P L^{-1} at the surface (0 m). This greater surface nutrient drawdown is accompanied by a further increase of $\delta^{15}N_{NO3}$ up to $7.8 - 8.8$ ‰ at 5 m and $9.6 - 11.0$ ‰ at 0 m. At the same time, there is a further drawdown of silicic acid towards the surface, but to a lesser extent than for nitrate and phosphate, falling to $33.97 - 40.36$ µmol L^{-1} at 5 m and $33.87 - 36.75$ µmol L^{-1} at the surface. The enhanced drawdown and isotopic enrichment towards the surface are not observed during lower productivity intervals between the two phytoplankton blooms or after the cessation of the phytoplankton bloom and associated nutrient uptake at the beginning of March (Fig. 2). Macronutrient concentrations and $\delta^{15}N_{NO3}$ at 100 m are representative of the winter water mass and reflect the variable degree and depth of mixing of WW with underlying UCDW and overlying AASW. As such, measured values fall between those of deep and surface waters at 25.2 ± 4.1 µmol N L^{-1}, 2.0 ± 0.2 µmol P L^{-1}, 56.4 ± 3.1 µmol Si L^{-1} and 5.6 ± 0.6 ‰ for nitrate, phosphate and silicic acid concentration, and $\delta^{15}N_{NO3}$ respectively.

Depth profiles of the molar ratio of dissolved inorganic nitrogen ($[NO_3^- + NO_2^- + NH_4^+]$) to phosphate ($[DIN]/[PO_4^{3-}]$) and silicic acid to DIN ($[Si(OH)_4^-]/[DIN]$) measured concurrently further reflect the differences in supply and utilisation of macronutrients with depth. Ammonium concentrations were only measured at 0 m and 15 m, so depth profiles of DIN and derived molar ratios are of lower resolution than the other profiles presented. Ammonium can be assumed to be negligible below the mixed layer, so $[NO_3^-]$ measured at or below 100 m can be treated as DIN. $[DIN]/[PO_4^{3-}]$ is 12.2 to 14.7 below 200 m and decreases to 9.0 to 14.4 at 15 m. During the times of higher production, $[DIN]/[PO_4^{3-}]$ declines dramatically above 15 m to values as low as $1.6 - 2.5$ at the surface, during the phytoplankton bloom in February, in concert with strong drawdown of nitrate and phosphate, and low $[NH_4^+]$ ($0.12 - 0.36$ µmol L^{-1}). In keeping with upper ocean variation in individual concentrations, $[DIN]/[PO_4^{3-}]$ does not show a pronounced decrease above 15 m during periods of lower productivity and after the cessation of the bloom. The $[DIN]/[PO_4^{3-}]$ ratio at 100 m (10.1 to 14.4) shows comparable variability to 15 m and 0 m data during low productivity times and greater variation than deeper values. $[Si(OH)_4^-]/[DIN]$ is 2.2 to 2.9 below 200 m, and increases in the upper ocean to $2.1 - 5.7$ at 15 m. During the phytoplankton bloom when surface drawdown of nitrate and silicic acid was greater than at 15 m, but to a lesser extent for silicic acid, $[Si(OH)_4^-]/[DIN]$ increased dramatically at the surface to high values (>25).

Similar to [DIN]/[PO$_4^{3-}$], this was not the case during lower productivity times or after the bloom had subsided. [Si(OH)$_4^-$]/[DIN] at 100 m was slightly more variable than deeper values, but broadly similar at 2.1 to 3.1. These nutrient and isotopic variations with depth show that primary production imparts a utilisation signature onto the surface waters, and that these nutrient utilisation signatures are imprinted to some extent onto WW due to vertical mixing with AASW.

3.4 Seasonal trends in UCDW and WW

Physical and nutrient data from 500 m depth, representative of the modified UCDW mass in Ryder Bay, show no major change in properties of this principal nutrient source over the 2009/10 season (Fig. 4). Potential temperature shows only a small increase, from 1.10 °C in mid-November to 1.16°C in mid-March, whilst salinity shows a negligible increase from 34.58 to 34.60 (Fig. 4a and b). During this time, nitrate concentration showed a small but non-monotonic increase from 32.46 μmol L^{-1} (when depth profile sampling began at the beginning of December) to 33.07 μmol L^{-1} by mid-March, concurrent with a decrease of δ^{15}N$_{NO3}$ from 5.3 to 4.7 ‰ (Fig. 4c). Phosphate concentration also increased from 2.40 to 2.71 μmol L^{-1}, reducing N* from -5.9 to -10.3 μmol L^{-1} (Fig. 4d). N* is calculated for WW and UCDW samples as N* = [NO$_3^-$ + NO$_2^-$] − 16[PO$_4^{3-}$], assuming negligible ammonium below the mixed layer. Over the sampling period, N* values for UCDW measured at 500 m were -8.73 ± 1.69 μmol L^{-1}. The small changes observed in UCDW in Ryder Bay are likely to integrate the effects of exchange with less-modified UCDW from further offshore on the WAP shelf, some degree of mixing with upper waters with partially-utilised nutrient signatures, and biogeochemical processes occurring in situ.

Physical and biogeochemical changes at 100 m are more pronounced than at 500 m and describe the properties of the temperature minimum (T$_{min}$) WW layer, as well as its definition and depth variation around 100 m driven by small variations in isopycnal depth. Depth profiles of potential temperature (Fig. 3d) describe the full water column context for the changes observed at 100 m (Fig. 4). Potential temperature increases gradually from -1.52 °C in mid-November to -0.84 on 22/2/10 when the surface phytoplankton bloom starts to subside, as the T$_{min}$ layer is eroded over the course of summer due to mixing with warmer waters above and below (Fig. 3d). The rapid temperature increase to 0.01 °C in mid-March (Fig. 4a) is accompanied by a decrease in salinity from 34.00 ± 0.05 until 22/2/10 to 33.79 by mid-March (Fig. 4b). Nitrate and phosphate concentrations and δ^{15}N$_{NO3}$ are variable over the

growing season (Fig. 4c and d), integrating the effects of nutrient uptake in surface waters, remineralisation of sinking organic matter and small changes in isopycnal depth which lead to varying influence of water masses above and below the T_{min}. Physical and nutrient changes at 100 m after the surface phytoplankton bloom demise in late-February reflect the downward propagation of low-nutrient surface waters, which are warm due to summer solar heating and low salinity due to meltwater inputs, driven by the onset of winter mixing [*Venables and Meredith*, 2014]. The observed biogeochemical changes in these sub-surface water masses are not sufficient to alter nutrient supply to phytoplankton, because macronutrient concentrations remained substantially higher than in surface waters throughout the growing season.

3.5 Nutrient uptake stoichiometry

The regression of nitrate versus phosphate concentration over the full water column depth for the entire study period ($r^2 = 0.871$, *p* <0.001) indicates close coupling of the nitrogen and phosphorus cycles, and the slope gives a net nitrate-to-phosphate uptake ratio of 12.9 ± 0.3 (Fig. 5a). Taking into account the relatively high concentrations of ammonium observed in the upper ocean, the net uptake ratio of DIN to phosphate ($[NO_3^- + NO_2^- + NH_4^+]/[PO_4^{3-}]$) is 12.3 ± 0.4 ($r^2 = 0.830$, *p* <0.001, Fig. 5a), since ammonium makes up a larger proportion of the DIN pool at lower $[NO_3^-]$. Both of these are lower than previous estimates for Ryder Bay based on upper ocean chlorophyll maximum (15 m) data alone (15.3; [*Clarke et al.*, 2008]), yet consistent with the overall mean N/P uptake ratio for the WAP, as reflected in the Palmer Antarctica Long-Term Ecological Research (Pal-LTER) region, of 14.42 ± 2.50, which shows no noticeable change latitudinally, spatially or during the growing season [*Pedulli et al.*, 2014]. Our $[NO_3^- + NO_2^- + NH_4^+]/[PO_4^{3-}]$ uptake ratio is also consistent with $\Delta N/\Delta P$ removal ratios calculated for Marguerite Bay from the US Southern Ocean Global Ecosystem Dynamics (SO GLOBEC) study in autumn 2001 (12.4 ± 1.6) and 2002 (11.1 ± 1.3) [*Serebrennikova and Fanning*, 2004]. $[DIN]/[PO_4^{3-}]$ uptake ratios lower than the Redfield ratio of 16N:1P in this region are likely driven by the documented prevalence of diatoms in this setting [*Annett et al.*, 2010; *Clarke et al.*, 2008], since diatoms have been shown to exhibit lower N/P ratios (9 – 13N:1P) than non-diatom phytoplankton (~19N:1P) in the Southern Ocean [*Arrigo et al.*, 1999; *Martiny et al.*, 2013; *Weber and Deutsch*, 2010]. Further, bloom-forming phytoplankton undergoing exponential growth have been found to allocate more resources to production of phosphorus-rich growth machinery (ribosomes),

lowering their N/P ratios [*Arrigo*, 2005; *Klausmeier et al.*, 2004]; our findings are also consistent with this mechanism.

In the current study, the ratio of [DIN]/[PO$_4^{3-}$] supplied to the surface ocean from UCDW (12.9 ± 0.9; Fig. 3f) is in excellent agreement with the ratio taken up by phytoplankton in the productive upper ocean (Fig. 5a). The N/P ratio of organic matter remineralisation can be estimated using upper ocean nutrient concentration changes in late summer 2009/10. From the beginning of bloom demise (22/2/2010) to the end of sampling in late March, near-surface DIN increased by 7.55 µmol L^{-1} whilst phosphate increased by 0.61 µmol L^{-1}. This translates to a N/P remineralisation ratio of 12.4. Although the N/P molar ratio of organic matter was not measured, conservation of the N/P ratio through nutrient supply, uptake and remineralisation implies that organic matter N/P was also ~12 – 13. Although we observe changes in N* in subsurface water masses during the growing season (Fig. 4d), this conservation of the N/P ratio strongly suggests that the nutrient stoichiometry of biological uptake and remineralisation does not impart a signature on the UCDW or WW over a complete annual cycle.

The regression of silicic acid versus nitrate concentration over the full water column depth for the entire study period shows a statistically significant yet weaker relationship than for [NO$_3^-$]/[PO$_4^{3-}$], with its slope giving a net uptake ratio of silicic acid to nitrate of 1.2 ± 0.1 (r^2 = 0.434, p <0.001; Fig. 5b). The net uptake ratio of silicic acid to DIN is 1.4 ± 0.1 (r^2 = 0.427, p <0.001). The weaker relationships are reflective of greater scatter in silicic acid concentrations, the one month offset in seasonal cycles and the greater drawdown of DIN in the uppermost surface ocean. Nevertheless, the relationship between silicic acid and DIN shows broad agreement between the seasonal dynamics of these two macronutrients and the derived Si/N uptake ratios strongly support diatom-dominated production in this setting [*Annett et al.*, 2010; *Clarke et al.*, 2008], in agreement with low N/P ratios. Diatom-dominated conditions are favoured by excess silicic acid being supplied to surface waters, as shown by the large positive intercept of the [Si(OH)$_4^-$]/[DIN] regression and mixed layer Si/N uptake ratios being lower than the [Si(OH)$_4^-$]/[DIN] ratio of the UCDW source (2.6 ± 0.3; Fig. 3g), creating a silicic acid-replete environment.

Whilst variability in ammonium concentrations is large and shows a role for ammonium recycling, particularly in the later summer and early autumn periods (Fig. 2f), similarity in N/P and Si/N ratios calculated with and without including [NH$_4^+$] indicates a relatively minor

role overall for ammonium-based production. The overall predominance of nitrate-based production is expected in a diatom-dominated community and consistent with an *f*-ratio of nitrate-based production vs. total production of 0.71-0.88 in this region [*Weston et al.*, 2013].

4. Interpretation and discussion

4.1 Isotopic insights into nutrient dynamics and nitrogen cycling

4.1.1 Nutrient source and vertical supply

High nutrient concentrations and low $\delta^{15}N_{NO3}$ at depth throughout summer 2009/10 (Fig. 3) are reflective of the modified UCDW nutrient source water mass, and its year-round presence across the WAP shelf. $\delta^{15}N_{NO3}$ of UCDW source waters here is in agreement with UCDW in the open Southern Ocean in the Pacific sector (5.0 ± 0.1 ‰, [*Rafter et al.*, 2013]), throughout the Antarctic zone interior in the Atlantic sector (4.83 ± 0.07 ‰, [*Smart et al.*, 2015]), and in the Antarctic zone in the east Pacific and east Indian sectors (5.2 ± 0.2 ‰, [*Sigman et al.*, 2000]). Macronutrient supply to Southern Ocean surface waters occurs primarily by wind- and buoyancy-induced vertical advective mixing over winter entraining deeper source waters into the upper ocean, as well as episodic mixing events and vertical diffusive flux during the summer. Vertical nutrient supply at the WAP is expected to be greater than in the open ocean due to shoaling of UCDW at the shelf break and its persistent presence up to ~200 m over the shelf [*Howard et al.*, 2004], as well as enhanced shelf mixing processes, coastal upwelling, internal wave activity, and larger diffusive flux driven by stronger nutrient concentration gradients [*Pedulli et al.*, 2014; *Prezelin et al.*, 2000; *Prezelin et al.*, 2004; *Wallace et al.*, 2008]. Mixing and upwelling processes are highly localised and temporally variable, and are regulated by local stratification, sea ice cover, winds, tides and bathymetry [*Dinniman and Klinck*, 2004; *Klinck*, 1998; *Smith and Klinck*, 2002; *Wallace et al.*, 2008]. Nutrient supply by wintertime vertical mixing in Ryder Bay is shown here by the similarity of macronutrient concentrations and N* between wintertime surface water values (Fig. 2) and UCDW values measured at 500 m (Fig. 4). Whilst the upper ocean in Ryder Bay is well-stratified during summer growing seasons in general, due to solar warming and meteoric and melt water inputs, episodic wind-induced mixing events are known to occur and are manifest here as transient increases in mixed layer depth (Fig. 2a).

4.1.2 Biological utilisation and modelling approaches

The drawdown of nitrate, phosphate and silicic acid and the increase in $\delta^{15}N_{NO3}$ into the surface ocean (Fig. 3) reflect biological utilisation of nutrients, supplied to the surface mixed layer by vertical mixing between UCDW, WW and AASW, by phytoplankton which discriminate against the heavier ^{15}N isotope. Nutrient utilisation is also observed in time-series data where $\delta^{15}N_{NO3}$ increases as nitrate concentration decreases, both from pre-bloom values similar to the UCDW source waters in most years, concurrent with increases in chlorophyll levels over the productive summer months (Fig. 2). Increases in N* in the early summer are also reflective of nutrient utilisation, as deep-sourced nitrate and phosphate are consumed in a ratio less than 16:1. However, the change in $\delta^{15}N_{NO3}$ relative to nitrate concentration is variable over the growing seasons and shows that nutrient utilisation, with its associated isotopic fractionation, is not the only process acting on these parameters.

Two contrasting models can be used to describe the relationship between $\delta^{15}N_{NO3}$ and nitrate concentration in time-series and depth profiles under different upper ocean conditions. The closed system or Rayleigh model dictates that a given nitrate source taken up with a constant isotope effect and with no nitrate resupply or dilution over the period of nitrate uptake [*Mariotti et al.*, 1981]. The open model describes a system in steady state, where nitrate is partially utilised with a constant isotope effect, and the supply of unutilised low-$\delta^{15}N$ nitrate is equal to the sum of biomass nitrogen produced and residual nitrate exported. The Rayleigh model is expected to be more applicable to the coastal WAP due to strong nutrient drawdown over summer in a well-stratified surface ocean with limited mixing, which leads to a high uptake/supply ratio and low nutrient concentrations in the surface ocean (<5 μmol NO_3^- L^{-1} in most years, Fig. 2c). The expectation of a closed system is supported further by the observation that winter mixing does not always fully resupply the surface ocean to nutrient concentrations equal to the source waters, e.g. in spring 2006 and 2008 (Fig. 2). In the WAP shelf setting, adherence to the closed system Rayleigh model requires that nitrate supply from the UCDW source and nitrate uptake by phytoplankton in the surface ocean are the only processes acting on $\delta^{15}N_{NO3}$ and nitrate concentration.

According to the Rayleigh model, the isotopic variation of nitrate as a given pool is progressively utilised is defined by

$$\delta^{15}N_{NO3^-} = \delta^{15}N_{NO3^-ini} - \varepsilon * \ln\left(\frac{[NO_3^-]}{[NO_3^-]_{ini}}\right) \qquad \text{Eq. 3}$$

where $\delta^{15}N_{NO3\ ini}$ and $[NO_3^-]_{ini}$ are the initial isotopic composition and concentration of the nitrate source and ε is the isotope effect of nitrate uptake. Whilst UCDW is the nutrient source for the entire WAP shelf, initial values are taken from WW ($\delta^{15}N_{NO3\ ini}$ = 5.6 ‰ and $[NO_3^-]_{ini}$ = 25.2 µmol L^{-1}), because this water mass sits immediately below AASW and supplies nutrients directly to the productive surface ocean. According to the Rayleigh model, the isotope effect of nitrate uptake is equal to the negative of the slope of the linear regression of $\delta^{15}N_{NO3}$ against the natural logarithm of nitrate concentration ($\ln[NO_3^-]$).

The isotope effect of nitrate assimilation for the polar Southern Ocean has been shown to be 5.0 ± 1.0 ‰ [*DiFiore et al.*, 2009; *Karsh et al.*, 2003; *Sigman et al.*, 1999a]. Figure 6 shows all data from this study plotted as $\delta^{15}N_{NO3}$ against $\ln[NO_3^-]$, as well as the modelled $\delta^{15}N$-$\ln[NO_3^-]$ relationships using initial values from WW and isotope effects of 4 ‰ and 5 ‰, which are at the low end of the range of published water column values. Our data consistently fall below modelled values in all years. Moreover, estimates of ε derived from our data for each season are consistently low (Fig. 6). These seasonal estimates were obtained from the $\delta^{15}N_{NO3}$-$\ln[NO_3^-]$ relationship between the season-maximum nitrate concentration and the following nitrate-minimum as the closest estimate to ε influenced by nitrate uptake alone. Extensive nitrate drawdown had already taken place when sampling commenced in summer 2009/10, so initial values were taken from the WW (100 m) sample on the first sampling event. Even despite this selective approach to estimating ε, each of our seasonal values is low with only one (2004/05) being within the range of published water column ε values, suggesting that these seasonal ε values are likely to be underestimating algal isotope fractionation. The deviation of our data from the Rayleigh model and the resultant underestimates of ε show that increases in $\delta^{15}N_{NO3}$ are small compared to nitrate drawdown, and strongly suggest that our data must be affected by other processes in addition to nutrient supply from UCDW and nitrate assimilation in surface waters, that lower $\delta^{15}N_{NO3}$ and violate the model. A similar deviation was also observed in Antarctic Peninsula shelf waters during the RITS '94 cruise in the South Pacific, suggesting that this is a pervasive feature in this region [*Sigman et al.*, 1999a]. Summertime resupply of unutilised nitrate from depth by episodic mixing events and/or vertical diffusive flux would not violate the model, because the reduction in $\delta^{15}N_{NO3}$ would be matched by an increase in nitrate concentration. This is shown by the fact that all data from WW, from which nutrients would be resupplied, plot on the modelled utilisation line in $\delta^{15}N$-$\ln[NO_3^-]$ space. As such, nutrient resupply would simply

move data points along the modelled line towards the initial values, and thus cannot explain the data-model deviation observed here.

The deviation of our data from the closed system model (Fig. 6) is quantified using the parameter $\delta^{15}N_{nr}$, which describes the difference between measured $\delta^{15}N_{NO3}$ and that predicted using the modelled utilisation-only trend [*Sigman et al.*, 1999a]. Non-Rayleigh (nr) fractionating processes are thus all those that cause deviations from the Rayleigh trend of nitrate utilisation of UCDW. Variations in $\delta^{15}N_{nr}$ can be driven by changes in $\delta^{15}N_{NO3}$ or nitrate concentration or both. We calculate $\delta^{15}N_{nr}$ using the minimum realistic ε value of 4 ‰, so that our data-model offsets are minimum estimates and can be used to examine the processes lowering $\delta^{15}N_{NO3}$ compared to the modelled $\delta^{15}N/\ln[NO_3^-]$ relationship. Using the minimum value of ε means that the lowering of $\delta^{15}N_{NO3}$ cannot be driven by changes in ε, which would have to be unrealistically low to achieve the $\delta^{15}N_{NO3}$ values observed here. Time-series data show that $\delta^{15}N_{nr}$ values are closest to zero at the beginning of each growing season after wintertime nutrient resupply by deep mixing, and become progressively more negative over the course of the summer as nitrate concentration decreases (Fig. 2i). Figure 6 also shows that data-model fit is better at higher nitrate concentration and the deviation increases as nitrate concentration decreases. A relationship with salinity is also observed whereby the deviation from the modelled utilisation curve is minimal at higher salinity and increases with decreasing salinity. This is supported by a statistically significant relationship between $\delta^{15}N_{nr}$ and salinity (p <0.001), which is strongest in the seasons following winters of longest-lived fast-ice cover, when sea-ice meltwater fraction showed a clear increase in surface waters during the summer ($r^2 = 0.574$, $p = 0.001$ in 2005/06; $r^2 = 0.548$, $p = 0.009$ in 2006/07). Good data-model fit in spring and early summer when nitrate and salinity are maximal suggests that utilisation of newly-supplied nitrate from depth is the dominant control on $\delta^{15}N_{NO3}$ early in the growing seasons. The increasing deviation as nitrate and salinity decrease implicates a process that lowers $\delta^{15}N_{NO3}$ and becomes more important as nitrate is drawn down over the summer season, or dilution of surface water nitrate by a source of low-salinity low-nitrate and/or low-$\delta^{15}N_{NO3}$ water, which exerts a greater effect at lower ambient nitrate concentration. The relationship with salinity strongly suggests a role for sea-ice meltwater, glacial meltwater and/or precipitation.

4.1.3 Dilution of surface water nitrate

In time-series data, changes in $\delta^{15}N_{nr}$ appear to correspond to changes in nitrate concentration rather than $\delta^{15}N_{NO3}$ (Fig. 2). With the observed relationship with salinity, this could imply that dilution of surface water nitrate by low-salinity low-nitrate water is the key process lowering $\delta^{15}N_{nr}$. Glacial meltwater and precipitation (collectively termed meteoric water) are expected to contain negligible nitrate, although this was not measured. Sea-ice meltwater is also expected to be significantly lower in nitrate than the seawater from which it was formed, due to intense nutrient drawdown by large accumulations of ice algae at the ice-ocean interface and from brine rejection during ice growth [*Fripiat et al.*, 2014]. A small number of samples collected in spring 2004 and 2005 show that nitrate concentration in sea ice in Ryder Bay is 3.64 ± 3.60 µmol L^{-1} [Henley et al., *in prep*]. Meteoric water has been shown to make a larger contribution than sea-ice meltwater to Ryder Bay surface waters [*Meredith et al.*, 2013], so can be expected to exert a greater dilution effect. Here we use known fractions of UCDW, meteoric water and sea-ice meltwater in Ryder Bay surface waters, derived from the oxygen isotope composition of seawater [*Meredith et al.*, 2013], with a representative nitrate concentration for each water source, to demonstrate that dilution of surface water nitrate concentrations alone cannot account for the observed changes in $\delta^{15}N_{nr}$. Nitrate concentrations of 33.0 µmol L^{-1} for UCDW, 0 µmol L^{-1} for meteoric water, and 3.6 µmol L^{-1} for sea-ice meltwater were input to the mixing model:

$$[NO_3^-] = f_{UCDW} * [NO_3^-]_{UCDW} + f_{MW} * [NO_3^-]_{MW} + f_{SIM} * [NO_3^-]_{SIM}$$

Where f_{UCDW} and $[NO_3^-]_{UCDW}$ are the fraction and nitrate concentration of UCDW, f_{MW} and $[NO_3^-]_{MW}$ are the fraction and nitrate concentration of meteoric water, and f_{SIM} and $[NO_3^-]_{SIM}$ are the fraction and nitrate concentration of sea-ice melt, respectively. The derived nitrate concentration for each sample was then subtracted from the nitrate concentration of UCDW to give a nitrate dilution effect, the maximum of which was 2.31 µmol L^{-1}. Measured nitrate concentrations were then corrected for the dilution effect to give the nitrate concentration for each sample when undiluted by meteoric or meltwater inputs. Seawater oxygen isotope data are only available for 15 m depth, so nitrate concentrations from other depths were normalised to the salinity of UCDW (34.60) as an alternative means of correcting for dilution. This is not as accurate as the corrections performed using meteoric and meltwater fractions and their nitrate concentrations, because salinity data cannot distinguish between low-salinity water sources, and because salinity normalisation assumes a salinity of zero for both meteoric and meltwater fractions. However, whilst sea-ice meltwater salinity is likely to be higher than zero and has been assigned a value of 7 in Ryder Bay [*Meredith et al.*, 2013],

the sea ice fraction is consistently smaller than the meteoric water fraction, which does have a salinity of 0, making this a reasonable assumption for the low-salinity end-member. For samples where both salinity and oxygen isotope data are available, the difference in the two dilution corrections is 0.83 ± 0.40 μmol L^{-1}. If dilution by meteoric and meltwater sources were the only process lowering $\delta^{15}N_{nr}$, these corrections would account for the changes in $\delta^{15}N_{nr}$ and bring our data into agreement with the Rayleigh model. Figure 7a shows that these corrections improve data-model fit, but our data still fall consistently below the modelled $\delta^{15}N/\ln[NO_3^-]$ line. This finding shows that dilution by meteoric and meltwater sources alone cannot account for the observed changes in $\delta^{15}N_{nr}$, and that biogeochemical processes additional to surface water nitrate utilisation must play a role.

4.1.4 Nitrification and correcting for nitrite interference

The isotopic composition of nitrite ($\delta^{15}N_{NO2}$) could have a significant effect on $\delta^{15}N_{NO3}$ as measured here ($\delta^{15}N$ of the combined nitrate+nitrite pool). *Smart et al.* [2015] have shown that $\delta^{15}N_{NO2}$ in the wintertime Antarctic mixed layer is very low (-20 to -40 ‰), and calculated the range of possible $\delta^{15}N$ values for a nitrite pool undergoing simultaneous production (by ammonium oxidation) and consumption (by nitrite oxidation) to be -34.8 to -14 ‰. Whilst nitrite concentrations were relatively low in general (<3 % of the nitrate+nitrite pool) during this study, the nitrite fraction increased markedly at low $[NO_3^-]$ (up to 20 % at $[NO_3^-]$ <1.5 μmol L^{-1}). Using the range of possible $\delta^{15}N_{NO2}$ values from *Smart et al.* [2015], nitrite would lower $\delta^{15}N_{NO3}$ values presented here by <0.4 ‰ to <0.9 ‰ at $[NO_3^-]$ >4 μmol L^{-1} and up to 2 ‰ to 5 ‰ at $[NO_3^-]$ <1.5 μmol L^{-1}. Using an intermediate value for $\delta^{15}N_{NO2}$ (-24 ‰) to correct our $\delta^{15}N_{NO3}$ data for nitrite interference increases $\delta^{15}N_{NO3}$ by 0.37 ± 0.48 ‰ with larger corrections at lower nitrate concentrations. As such, correcting for nitrite interference increases $\delta^{15}N_{nr}$ and improves the fit of the data to the Rayleigh model. Figure 7b shows the relationship between $\delta^{15}N_{NO3}$ data corrected for nitrite interference and $\ln[NO_3^-]$ corrected for dilution by low-salinity meteoric and meltwaters, in order to show the extent to which our data agree with the Rayleigh model once the effects of both of these phenomena have been removed. Robust utilisation trends are found for all summers, using initial values and a subset of values for each season which best reflect isotope fractionation during utilisation alone, with isotope effects of 4.19 ± 0.29 ‰. These estimates are in agreement with previous findings in the polar Antarctic zone, where nitrite corrections to $\delta^{15}N_{NO3}$ data (also measured as $\delta^{15}N$ of nitrate+nitrite) were not required due to low contributions of nitrite to the total nitrate+nitrite pool [*DiFiore et al.*, 2009; *Sigman et al.*, 1999a]. The nitrite

correction made here is required for our $\delta^{15}N_{NO3}$ data because our nitrate concentrations reached substantially lower levels than in the previous studies, such that the nitrite contribution to the combined pool was much higher. In all seasons during this study there remains significant deviation from observed and modelled utilisation trends in a large number of samples after correction for dilution and nitrite interference, with the deviation being larger at lower nitrate concentration. The relationship between $\delta^{15}N_{nr}$ and salinity becomes statistically insignificant (p >0.05) in most seasons and considerably weaker in 2005/06 (r^2 = 0.2974, p = 0.0355) as a result of these corrections. The remaining deviation is not driven by changes in surface nitrate concentrations due to dilution by low-salinity waters, or nitrite interference, and must instead be driven by a lowering of $\delta^{15}N_{NO3}$ by one or more biogeochemical processes at work. Candidate processes responsible for this lowering include nitrification in the water column, intense nitrogen uptake and recycling in sea ice, and lateral exchange between different water masses affecting the $\delta^{15}N/[NO_3^-]$ properties of the T_{min} layer nutrient source. Of these, we argue that water column nitrification is the process most likely to be driving the lowering of $\delta^{15}N_{NO3}$ that we observe.

Water column nitrification during summer phytoplankton blooms and winter periods has been found to lower $\delta^{15}N_{NO3}$ in Antarctic waters [*Fripiat et al.*, 2015b; *Smart et al.*, 2015]. Intense nitrogen recycling is indicated in this study by relatively high concentrations of ammonium and nitrite from mid-summer into autumn and reductions in N* in the autumn, reflective of remineralisation of organic matter with a N/P ratio lower than the Redfield ratio. The accumulation of ammonium in the mixed layer from summer into autumn shows that ammonium uptake by phytoplankton is outpaced by ammonium release from decaying organic matter, such that a pool of ammonium is available for nitrification. Nitrification produces nitrate with low $\delta^{15}N_{NO3}$ compared to the deep water source due to isotope fractionation during nitrate uptake, PN degradation, and ammonium regeneration. The isotope effect of the first step of nitrification (ammonium oxidation: ε = 12 to 19 ‰ [*Casciotti et al.*, 2003]) is largely offset by the inverse isotope effect of the second step (nitrite oxidation: ε = -13 ‰ [*Casciotti*, 2009]). As such, $\delta^{15}N$ of nitrate produced by nitrification is similar to or lower than that of isotopically light ammonium released from decaying organic matter. Low-$\delta^{15}N$ nitrified nitrate would have a greater effect on surface ocean $\delta^{15}N_{NO3}$ at lower ambient nitrate concentrations, such that water column nitrification is consistent with the observation that $\delta^{15}N_{nr}$ is close to 0 ‰ at high $[NO_3^-]$ and becomes increasingly negative with decreasing $[NO_3^-]$ (Fig. 2 and 7b). The net isotope effect produced

by assimilation and nitrification would thus be lower than that produced by assimilation alone; for example, a net isotope effect of 3.0 ± 0.3 ‰ was found during the naturally iron-fertilised bloom in the deep mixed layer over the southeast Kerguelen Plateau, where nitrification accounted for ~40-80 % of seasonal nitrate uptake [*Fripiat et al.*, 2015b].

Nitrification requires low light levels for nitrifiers, which are partly photo-inhibited, to outcompete phytoplankton (photo-limited) for the available ammonium. Nitrification during the phytoplankton bloom over the southeast Kerguelen Plateau was attributed to sufficiently low light levels in the deep mixed layers during summer [*Fripiat et al.*, 2015b]. Maximum nitrification rates are known to occur at the base of the euphotic layer, where PAR is 1-10 % of its surface value [*Fripiat et al.*, 2015b; *Ward*, 2008]. In the sea ice zone, the depth of the euphotic layer is partly regulated by sea ice coverage because ice causes much greater attenuation of light than seawater. However, sea ice coverage is minimal during the summer seasons of this study (Fig. 2a), so the effect on PAR is expected to be small. Here we use the depth at which PAR is 5 % of its surface value as an indicator of where nitrification is most likely to be occurring in the water column during austral summer (Fig. 2a). We hypothesise that if mixed layer depth is deeper than the 5 % PAR depth, nitrification would be promoted in the lower part of the mixed layer, and/or biogeochemical signatures from nitrification at the base of the euphotic layer just below the mixed layer can be entrained into the mixed layer itself. Figure 2a shows that whilst the 5 % PAR depth is deeper than MLD over most of the summer growing seasons, such that the mixed layer is shallow and well-lit for the most part and mixed layer nitrification is thus unlikely, episodic mixing events lead to MLD being deeper than the 5 % PAR depth. This incursion of the mixed layer into the horizon of light levels most favourable for nitrification promotes the likely influence of nitrification within and/or just below the mixed layer on lowering $\delta^{15}N_{NO3}$ measured in the upper ocean in this study. Variability in $\delta^{15}N_{NO3}$ in the winter water mass over summer 2009/10 also indicates coupled organic matter remineralisation and nitrification in overlying waters, as the only process capable of lowering $\delta^{15}N_{NO3}$ compared to the UCDW source value (Fig. 4), as well as downward propagation of surface water utilisation signals which increases $\delta^{15}N_{NO3}$. In 2008/09, $\delta^{15}N_{nr}$ in the mixed layer shows a marked reduction over the summer, which is driven by a similar reduction in $\delta^{15}N_{NO3}$ with little change in nitrate concentration (Fig. 2). This lowering of $\delta^{15}N_{NO3}$ is also most likely to be caused by water column nitrification occurring concurrently with nitrate utilisation or a gradual input of nitrate bearing a low-$\delta^{15}N$ signature from nitrification. The influence of nitrification is supported by the gradual increase

in nitrite concentration over summer 2008/09. Whilst MLD is deeper and more variable in summer 2008/09 than the other years examined, potentially favouring mixed layer nitrification, the 5 % PAR depth is also greater overall, such that the mixed layer rarely incurs into the horizon of maximum nitrification (Fig. 2a). Mixed layer nitrification thus appears no more likely in 2008/09 than in the other summer seasons, such that the nitrification signature is more likely to derive from beneath the mixed layer at the base of the euphotic layer, and be entrained into the mixed layer by a greater degree of mixing overall in this year, as indicated by greater mixed layer depths.

Nitrification is also likely to occur in the winter mixed layer [*Smart et al.*, 2015], which is comparatively deep as a result of enhanced winter mixing and poorly-lit due to low insolation and the presence of sea ice causing greater light attenuation than seawater. As the study location is within the polar circle, sunlight is absent during the midwinter period (approximately 1 month from early June to early July), and surface PAR is highly variable and substantially lower than outside the polar circle from late autumn to early spring. As such, the 5 % PAR depth which coincides with maximum nitrification rates outside the polar circles [*Ward*, 2008] and in the polar summers becomes meaningless, so is not used to indicate the depth where nitrification is most likely from April to September in this study (Fig. 2a). Nevertheless, nitrification is likely to occur in the mixed layer during this time, due to deeper mixing coupled with low insolation creating favourable light conditions for nitrifiers. Whilst isotopic data are not available, wintertime mixed layer nitrification is suggested here by reductions in ammonium concentration over most winter periods examined, when ammonium uptake by phytoplankton is expected to be minimal (Fig. 2). Being partially light-inhibited, nitrification would not be expected during the short midwinter period when incoming light is zero, although wintertime sampling resolution was not sufficient to examine this feature. Wintertime mixed layer nitrification only has a small effect on $\delta^{15}N_{nr}$ in springtime surface ocean samples from 2005, 2006 and 2008, and no effect in 2004 and 2009 or on $\delta^{15}N_{NO3}$ in the winter water mass in 2009, because the low-$\delta^{15}N_{NO3}$ signature from nitrification is overprinted to a large extent by deep-sourced nitrate supplied by wintertime mixing between AASW, WW and UCDW. This suggests that water column nitrification in the lower part of the euphotic zone during summer is more important than wintertime nitrification in driving the lowering of mixed layer $\delta^{15}N_{NO3}$ observed in this study, and can explain the increasing effect of low-$\delta^{15}N$ nitrified nitrate on $\delta^{15}N_{nr}$ as nitrate is drawn down during summer.

Nitrification has also been shown to be significant in Antarctic sea ice [*Fripiat et al.*, 2015a] and can cause a lowering of $\delta^{15}N_{NO3}$ within the ice matrix [*Fripiat et al.*, 2014]. Nitrate assimilation in sea ice can proceed with a range of organism-level ε values, depending on physiological responses of sea-ice algae to variable light levels [*DiFiore et al.*, 2010; *Fripiat et al.*, 2015a]. However, the effect of this variability on $\delta^{15}N_{NO3}$ can be overprinted by low-$\delta^{15}N$ nitrate from sea ice nitrification, which causes an overall lowering of $\delta^{15}N_{NO3}$ compared to utilisation alone, and could impact on surface water N isotope biogeochemistry as a result of ice-ocean exchange processes and/or ice melting. Whilst sea-ice brine and meltwater are input to the surface ocean in Ryder Bay, their $\delta^{15}N_{NO3}$ signatures are unlikely to influence surface water N isotope biogeochemistry. This is because sea-ice primary production occurs with a high degree of nitrate utilisation within the semi-closed sea ice matrix by large accumulations of algae at the ice-ocean interface, such that concentrations of isotopically fractionated nitrate and thus their contribution to the underlying surface ocean are very low. Isotope mass balance calculations based on oxygen isotope-derived sea-ice meltwater fractions, measured $[NO_3^-]$ and $\delta^{15}N_{NO3}$ in surface waters, and measured and theoretical values for $[NO_3^-]$ and $\delta^{15}N_{NO3}$ in sea ice are used to illustrate the minor effect of low-$\delta^{15}N$ nitrate from sea ice on surface water $\delta^{15}N_{NO3}$ during this study, according to:

$$\delta^{15}N_{NO3} = f[NO_3^-]_{SIM} * \delta^{15}N_{NO3\,SIM} + f[NO_3^-]_{SW} * \delta^{15}N_{NO3\,SW}$$

$f[NO_3^-]_{SIM}$ and $f[NO_3^-]_{SW}$ are the fractions of nitrate derived from sea-ice meltwater and seawater, respectively, and are calculated using the oxygen isotope-derived sea-ice meltwater fraction, measured surface water $[NO_3^-]$ values and $[NO_3^-]$ measured in sea ice in Ryder Bay (3.6 µmol L^{-1} [Henley et al., *in prep*]). $\delta^{15}N_{NO3\,SIM}$ is the isotope composition of nitrate derived from sea-ice meltwater and is taken from the lowest value measured in Ryder Bay sea ice (0.3 ‰ [Henley et al., *in prep*]) and a theoretical minimum value based on all nitrate being newly nitrified within the sea ice matrix (-13 ‰ [*Fripiat et al.*, 2014]). $\delta^{15}N_{NO3\,SW}$ is the isotope composition of nitrate in seawater that is derived from seawater only, i.e. not from sea ice inputs, and is calculated using measured surface water $\delta^{15}N_{NO3}$ and the mass balance equation. This approach assumes that meteoric water does not act as a nitrate source to surface waters [*Dierssen et al.*, 2002; *Karl et al.*, 2002; *Pedulli et al.*, 2014]. Using the minimum $\delta^{15}N_{NO3\,SIM}$ measured in Ryder Bay sea ice (0.3 ‰), the effect of low-$\delta^{15}N$ nitrate from nitrification in sea ice on surface waters is undetectable (<0.02 ‰). Using the theoretical minimum value for newly nitrified sea-ice nitrate (-13 ‰), the maximum lowering of surface water $\delta^{15}N_{NO3}$ by sea ice inputs is 0.42 ‰ with the majority of values being ≤0.12

‰. Even when using these minimum sea ice values to calculate the maximum effect of sea ice nitrification on surface water $\delta^{15}N_{NO3}$, low-$\delta^{15}N$ nitrate from sea ice does not cause a significant lowering of surface water $\delta^{15}N_{NO3}$ and cannot account for the observed $\delta^{15}N_{nr}$ values. This is due to low nitrate concentrations in the thin sea ice cover, which make a very minor contribution to the surface nitrate inventory compared to the deep nutrient-rich ocean below, such that sea-ice $\delta^{15}N_{NO3}$ does not have an appreciable effect on the isotope composition of surface nitrate. The principal influence of sea ice on surface water nitrate is then dilution by low-nitrate meltwaters, alongside meteoric waters, which lowers surface water nitrate concentration, but has negligible effect on $\delta^{15}N_{NO3}$. Whilst the dilution of surface water nitrate acts to reduce estimates of net isotope effect, as explained above, this mechanism only accounts for relatively small changes in $\delta^{15}N_{nr}$ during this study, such that sea ice processes are not the main drivers of low $\delta^{15}N_{NO3}$ that we observe. This is particularly the case in the later years of the study (2008-10), when winter sea ice was short-lived and sea-ice meltwater fraction showed little increase in surface waters over the summer months (Fig. 2).

The negligible effect of sea ice nitrification on surface water $\delta^{15}N_{NO3}$ strongly supports the argument for water column nitrification being the primary non-Rayleigh fractionating process driving the large variations of $\delta^{15}N_{nr}$ that we observe. Further, our estimates of net isotope effect (Fig. 6) are similar to the low values (< 4 ‰) reported in the open Southern Ocean during summer [*Fripiat et al.*, 2015b] and winter periods [*Smart et al.*, 2015] that have been attributed to mixed layer nitrification. Good agreement between these values reported where no sea ice was present and our data further supports the hypothesis that water column nitrification plays a key role in lowering $\delta^{15}N_{NO3}$ in this coastal Southern Ocean study. Future work using the dual nitrogen and oxygen isotope composition of nitrate will provide more detailed insight into nitrification in the water column and sea ice in this region.

4.1.5 Lateral exchange and connectivity

One remaining mechanism that could drive the observed lowering of $\delta^{15}N_{NO3}$ in Ryder Bay and has been observed in the Southern Ocean is lateral exchange between different water masses affecting the $\delta^{15}N/[NO_3^-]$ properties of the T_{min} layer nutrient source [*DiFiore et al.*, 2010]. In the sub-Antarctic, lateral advection of surface water masses has also been shown to affect the surface ocean $\delta^{15}N/[NO_3^-]$ signature, as a result of the different $\delta^{15}N/[NO_3^-]$ relationships of different nutrient sources: UCDW supplied to surface waters in the Antarctic

zone and then advected northwards, and the local sub-Antarctic thermocline [*Sigman et al.*, 1999a; *Tuerena et al.*, 2015]. At the WAP, UCDW is the nutrient source to the entire shelf year-round [*Dinniman et al.*, 2011; *Martinson and McKee*, 2012; *Moffat et al.*, 2009], such that lateral exchange would not affect the nutrient source water mass or its $\delta^{15}N/[NO_3^-]$ properties. This is shown by T_{min} layer data sitting on the utilisation/mixing trend between UCDW and surface waters (Fig. 6). These findings are in agreement with those from the polar Antarctic zone south of Australia [*DiFiore et al.*, 2010], and show that lateral exchange between different water masses cannot account for the lowering of $\delta^{15}N_{NO3}$ observed in Ryder Bay.

Lateral advection of surface waters with $\delta^{15}N/[NO_3^-]$ properties modified from the UCDW source signature could contribute to the lowering of our $\delta^{15}N_{NO3}$ data compared to the Rayleigh model, given the strong shelf and coastal currents that distribute physical and biogeochemical properties over areas much larger than Ryder Bay [*Klinck et al.*, 2004; *Savidge and Amft*, 2009; *Wallace et al.*, 2008]. As such, the processes that we have identified as potential modifiers of the $\delta^{15}N/[NO_3^-]$ properties of surface waters in Ryder Bay – dilution by meteoric and meltwaters, and water column nitrification – are likely to be at work upstream of the sampling location as well as in Ryder Bay. The APCC flows southwestwards down the WAP coast with a presumed cyclonic circulation within Marguerite Bay [*Beardsley et al.*, 2004; *Moffat et al.*, 2008; *Savidge and Amft*, 2009], and surface waters are thought to exchange openly between Marguerite Bay and Ryder Bay (see section 4.3). This being the case, the $\delta^{15}N/[NO_3^-]$ properties of surface waters in Ryder Bay are likely to integrate processes occurring in coastal regions further north along the WAP, as well as in Marguerite and Ryder Bays. As such, our results may be applicable to WAP shelf surface waters further afield than just Ryder Bay.

4.1.6 Upper ocean mixing and isotope systematics

Mixed layer depth exerts a strong control on nutrient biogeochemistry and N isotope systematics throughout this study. In the coastal WAP, sea ice coverage during the winter and early spring regulates the degree of stratification and mixed layer depth during the winter and into summer, with important implications in the context of contemporary climate change [*Saba et al.*, 2014; *Venables et al.*, 2013]. Long-lived winter fast-ice reduces the transfer of momentum between the atmosphere and the ocean, increasing stratification and reducing MLD. This preconditioning persists into spring and summer, and stratification is enhanced

further by springtime meltwater inputs. Short-lived winter fast-ice cover leaves the surface ocean exposed to intense winds and leads to strong air-sea buoyancy fluxes, reducing stratification and increasing mixed layer depth, which persist into spring and summer. Sea ice-induced changes in MLD may have important implications for nutrient supply, primary production and nutrient uptake, fractionation of nitrogen isotopes, and nitrification in the lower part of the euphotic layer.

Latitudinal changes in ε in the Southern Ocean have been found to correlate strongly with changes in mixed layer depth due to the physiological response of diatoms to the light environment, with lower light availability in deep mixed layers leading to higher cellular efflux of nitrate and higher organism-level ε [*DiFiore et al.*, 2010]. Consistent with this relationship, shallow well-lit mixed layers observed during summers in Ryder Bay compared to the open Southern Ocean may explain our ε values towards the lower end of the range of published water column values, in agreement with previous findings from the polar Antarctic zone [*DiFiore et al.*, 2009]. In contrast, the lowering of $\delta^{15}N_{NO3}$ relative to utilisation trends that we observe cannot be explained by changes in organism-level ε related to mixed layer depth, which would lead to higher ε and $\delta^{15}N_{NO3}$ in the deeper mixed layers of summer 2008/09 and 2009/10 [*DiFiore et al.*, 2010]. In fact, $\delta^{15}N_{NO3}$ is lower than expected from utilisation in all years of this study, and our estimates of net seasonal ε based on corrected $\delta^{15}N_{NO3}$ and $[NO_3^-]$ data from a subset of samples were not significantly different between summers of shallow (2004/05, 2005/06, 2006/07) and deeper (2008/09, 2009/10) mixing (Fig. 2a and 7b). These findings show that the relationship between ε and mixed layer depth [*DiFiore et al.*, 2010] is not expressed in our seasonal data, either because other processes have a larger effect on $\delta^{15}N_{NO3}$ and nitrate concentration, or because interannual variability in mixed layer depth was not sufficient to drive appreciable changes in ε. We invoke water column nitrification at the base of the euphotic layer, just below or within the deeper part of the mixed layer, as the process most likely to be causing the lowering of $\delta^{15}N_{NO3}$ and estimates of ε, in agreement with open ocean studies [*Fripiat et al.*, 2015b; *Smart et al.*, 2015]; this effect of nitrification overprints the influence of MLD, via light, on the organism-level isotope effect [*DiFiore et al.*, 2010] in our $\delta^{15}N_{NO3}$ data.

Water column nitrification is itself influenced strongly by mixed layer depth and its relationship with euphotic depth [*Fripiat et al.*, 2015b], as explained above. Indeed, the pronounced effect of nitrified nitrate on upper ocean $\delta^{15}N_{NO3}$ over summer 2008/09 may be related to MLD since deeper mixing in this year likely caused greater entrainment of the low

$\delta^{15}N_{NO3}$ nitrification signature into the upper mixed layer. As such, variability in MLD also affects the surface ocean supply of newly nitrified nitrate from the lower euphotic layer. Mixed layer depth is also expected to regulate the supply of new nitrate from underlying source water masses and the nitrate supply/uptake ratio, with enhanced supply during years of deeper mixing. Interannual variability in nutrient supply is not assessed during this study as nutrient depth profile data are only available for one year, but this is the subject of ongoing work in Ryder Bay.

Changes in sea ice and mixed layer depth also exert a strong control on primary production and nutrient uptake in the coastal WAP setting [*Saba et al.*, 2014; *Venables et al.*, 2013]. This control and the implications of ongoing changes in sea ice and coupled upper ocean processes for primary production, nutrient dynamics and isotope systematics are discussed in section 4.3.

4.2 Nutrient uptake and primary production

Net seasonal nitrate drawdown over the entire euphotic surface layer for summer 2009/10 in Ryder Bay was 1.83 mol N m^{-2} yr^{-1}. This value was calculated from full-depth nutrient profiles as the difference between maximum 100 m-integrated nitrate concentration during the winter and the minimum concentration measured at the peak of the bloom. This is a minimum value since it does not account for mid-season nutrient resupply driven by episodic wind-driven mixing events. All measured values were normalised to the salinity of the UCDW nutrient source (34.60) to account for the dilution of surface water nitrate by low-nitrate freshwater inputs. Because no depth profile measurements were made during the winter when measured near-surface (15 m) values were maximal (28/10/2009; Fig. 2c), we assume that the measured value (31.71 µmol L^{-1}) was representative of the upper water column down to 100 m due to the strong vertical winter mixing required to supply high nitrate concentrations to the surface. The peak bloom minimum 100 m-integrated nitrate concentration (1.39 mol N m^{-2}) was calculated from salinity-normalised measured water column values and was subtracted from the salinity-normalised winter value (3.22 mol N m^{-2}) to give the seasonal drawdown value of 1.83 mol N m^{-2} yr^{-1}. This net seasonal drawdown value is substantially greater than that based on autumn values for Marguerite Bay in 2001 and 2002 (~0.6 mol N m^{-2} yr^{-1} [*Serebrennikova and Fanning*, 2004]), likely because nutrient resupply to the surface layer after the peak of the phytoplankton bloom compensates for some degree of summer nutrient drawdown such that autumn values do not capture the annual

minimum nutrient concentrations. Using our estimate of seasonal nitrate drawdown, which does capture the annual minimum, and the Redfield ratio of 106C:16N, net seasonal carbon uptake by phytoplankton was estimated to be 12.1 mol C m^{-2} yr^{-1} or 146 g C m^{-2} yr^{-1}. These values for summer 2009/10 are consistent with nutrient deficit-derived exportable production values for Ryder Bay estimated for 2005-06 using a similar nutrient drawdown approach [*Weston et al.*, 2013], and in broad agreement with primary production in Marguerite Bay from ^{14}C-uptake experiments from the Pal-LTER project between 1995 and 2006 [*Vernet et al.*, 2008]. Spatial variability throughout the WAP region is distinct, such that values for Marguerite Bay are higher than comparable estimates of primary production for the coastal region further north along the WAP (65 to 67°S) [*Ducklow et al.*, 2012], and that the mean of all coastal values (including Marguerite Bay) is substantially higher than those from WAP shelf and slope regions deeper than 450 m [*Pedulli et al.*, 2014].

High primary productivity in this WAP coastal region is facilitated by stratified upper ocean conditions that are required for large phytoplankton blooms to form [*Venables et al.*, 2013] and availability of sufficient macro- and micro-nutrients. Vertical mixing with nutrient-rich subsurface waters creates a silicic-acid replete environment, and this coupled with adequate iron supply (both shown by the Si/N uptake ratio [*Franck et al.*, 2000; *Hutchins and Bruland*, 1998; *Mosseri et al.*, 2008; *Takeda*, 1998]) promotes large diatom blooms characteristic of Marguerite Bay [*Annett et al.*, 2015; *Garibotti et al.*, 2003]. Iron-replete conditions have been shown directly in Ryder Bay, with iron being supplied to surface waters from the interaction of UCDW with iron-rich shelf sediments and from glacial sources during summer growing seasons [*Annett et al.*, 2015]. Observed seasonal changes in the biogeochemical properties of UCDW and WW were not sufficient to affect macronutrient supply to surface phytoplankton blooms. Diatom-dominated primary production causes a net drawdown of CO$_2$ into organic carbon which can be exported from the mixed layer, such that the large phytoplankton blooms observed in Ryder Bay and elsewhere over the WAP shelf have the potential to drive carbon sink behaviour [*Carrillo et al.*, 2004; *Legge et al.*, 2015; *Montes-Hugo et al.*, 2010; *Ruiz-Halpern et al.*, 2014].

Vertical profiles from summer 2009/10 (Fig. 3) offer a mechanistic insight into the vertical structure of the phytoplankton bloom in Ryder Bay and its biogeochemical consequences. Whilst we cannot assume *a priori* that these more detailed findings are representative of all growing seasons, the maximal macronutrient drawdown above 15 m depth, consistent with supply from depth, a stratified surface ocean and greatest uptake by phytoplankton in the

uppermost surface ocean, is unlikely to be applicable to this year alone. The depth interval of greatest nutrient uptake varies between $15 - 10$ m, $10 - 5$ m and $5 - 0$ m, strongly suggesting that the depth of maximum phytoplankton production is variable but consistently above 15 m throughout the course of the bloom. The shallow phytoplankton bloom is likely to be associated with the surface freshwater lens formed from spring/summer inputs of sea-ice and glacial meltwater. In years when fast-ice is present in Ryder Bay during the phytoplankton bloom, near-surface nutrient drawdown may be enhanced further by intense ice algal primary production at the ice-ocean interface. However, fast-ice was not present in Ryder Bay during summer 2009/10 (Fig. 2a), so the observed near-surface nutrient drawdown was unrelated to sea-ice biology.

We have shown that nitrate and phosphate are drawn down above 15 m to a greater extent than silicic acid during the phytoplankton bloom (Fig. 3). This is consistent with the $[Si(OH)_4^-]/[DIN]$ uptake ratio at the surface (0.6 ± 0.1, $r^2 = 0.780$, $p < 0.001$) being significantly lower than at 15 m (0.9 ± 0.1, $r^2 = 0.732$, $p < 0.001$). This observation could be driven by nutrient uptake by non-siliceous phytoplankton, as well as diatoms, in the uppermost surface ocean, and/or remineralisation of organic matter occurring at a greater rate than the dissolution of diatom frustules [*Dugdale et al.*, 1995] and this process being more important at the surface than at 15 m. The $[Si(OH)_4^-]/[DIN]$ uptake ratio for the whole upper ocean (<100 m) in summer 2009/10 is 0.7 ± 0.08 ($r^2 = 0.743$, $p < 0.001$), which is lower than the overall value for the study (1.4 ± 0.1, Fig. 5b) and suggests that the role for non-siliceous phytoplankton and/or remineralisation was more important during 2009/10 than in other seasons. The lower $[Si(OH)_4^-]/[DIN]$ uptake ratio above 15 m further suggests that one or both of these factors was most important in the uppermost surface ocean. The $[DIN]/[PO_4^{3-}]$ uptake ratio for all upper ocean data from summer 2009/10 (15.8 ± 0.5, $r^2 = 0.959$, $p < 0.001$) was higher than the overall study value (12.3 ± 0.4), and was indistinguishable between the surface (15.9 ± 0.5, $r^2 = 0.989$, $p < 0.001$) and 15 m (15.5 ± 1.1, $r^2 = 0.903$, $p < 0.001$). This convergence on the Redfield ratio indicates a mixed phytoplankton assemblage comprising diatoms (N/P <16) and non-siliceous phytoplankton (N/P >16) throughout the mixed layer [*Arrigo et al.*, 1999; *Martiny et al.*, 2013; *Weber and Deutsch*, 2010]. The $[DIN]/[PO_4^{3-}]$ uptake ratio being indistinguishable between 15 m and the surface suggests that there is no significant difference in the contribution of diatom versus non-diatom phytoplankton species between the two depths, so the fact that $[Si(OH)_4^-]/[DIN]$ is significantly lower at the surface

than at 15 m is likely driven by greater surface remineralisation rates, which proceed at a faster rate than biogenic silica dissolution [*Dugdale et al.*, 1995].

Strong drawdown of DIN relative to silicic acid and to a lesser extent phosphate between 15 m and the surface during the phytoplankton bloom in summer 2009/10 (see $[Si(OH)_4^-]/[DIN]$ and $[DIN]/[PO_4^{3-}]$ molar ratios in Fig. 3) shows that intense nutrient drawdown in the uppermost surface ocean has the potential to drive nitrogen limitation in and just below the surface freshwater lens. Such nutrient limitation has been observed previously in Marguerite Bay [*Dore et al.*, 1992] and other high-productivity iron-replete Antarctic coastal regions [*Alderkamp et al.*, 2012; *Gerringa et al.*, 2012]. However, nutrient concentration data show that nitrogen limitation was rare and short-lived during this study, before nitrate and/or ammonium were regenerated in situ or resupplied from deeper waters or by lateral advection.

The substantial macronutrient drawdown by a mixed phytoplankton assemblage in the uppermost surface ocean strongly suggests that there was also a strong drawdown of CO_2 at the ocean surface that is not observed at or below 15 m. As such, primary production and CO_2 uptake in the upper ocean in coastal regions like Ryder Bay are likely to be higher than previously inferred based on 15 m data alone.

A further biogeochemical consequence of the mixed phytoplankton assemblage observed in summer 2009/10 may be species-specific variations in the nitrogen isotope effect associated with uptake by diatom and non-diatom groups, which could affect seasonal values of ε. However, such species effects cannot explain the lowering of measured $δ^{15}N_{NO3}$ values compared to modelled values shown here because the latter were based on the minimum ε value for the polar Southern Ocean (4.0 ‰), so any lowering of $δ^{15}N_{NO3}$ due to inter-specific variations in organism-level ε was accounted for in the modelling approaches (see section 4.1).

4.3 Interannual variability in nutrient uptake and potential future changes

Over the five year time-series, we observed distinct interannual variability in Ryder Bay, which is characteristic of Antarctic sea ice zones [*Clarke et al.*, 2008]. Near-surface macronutrient concentrations and nitrate isotope signatures show strong nutrient drawdown and isotopic enrichment during summers 2004/05, 2005/06, 2006/07 and 2009/10, but much less drawdown and a lack of isotopic enrichment over summer 2008/09 (Fig. 2). It is not possible to assess quantitatively the interannual variability in seasonal nitrate drawdown since

depth profile data are only available for 2009/10. However, we can compare seasonal average $\delta^{15}N_{NO3}$ values from 15 m to assess qualitatively the interannual variability in nutrient utilisation between 2004 and 2010 (Table 1). Average $\delta^{15}N_{NO3}$ for 2004/05, 2005/06, 2006/07 and 2009/10 is higher than the UCDW source value (4.9 ± 0.4 ‰) by ≥2 ‰, whilst that for 2008/09 is, at 5.3 ‰, only slightly higher than the UCDW source. A series of Welch two-sample t-tests on time-series data shows that the difference between 2008/09 and all other years was statistically significant ($p \ll 0.05$) in terms of $\delta^{15}N_{NO3}$ (Table 1). We have shown here that $\delta^{15}N_{NO3}$ is influenced by factors additional to nitrate utilisation, which may affect these seasonal variations. For instance, water column nitrification appears to affect $\delta^{15}N_{NO3}$ values to a greater extent in 2008/09 than the other seasons, so could be at least partly responsible for the low seasonal average value. However, interannual variability in $\delta^{15}N_{NO3}$ is consistent with upper ocean macronutrient and chlorophyll data, and this strongly suggests that nutrient utilisation was significantly lower during 2008/09 than in any other year studied. *Venables et al.* [2013] showed that the marked decrease in summertime chlorophyll levels in Ryder Bay between 2007 and 2010, with particularly low chlorophyll conditions in 2008/09, was driven by reduced fast-ice duration and a resultant shift to deeper mixed layers during the preceding winter, followed by conditions of reduced spring/summer stratification (Fig. 2). Less stratified conditions are unfavourable for large phytoplankton blooms because phytoplankton cells are mixed over a greater depth range, thus being exposed to highly variable light levels, which reduces photosynthetic efficiency and limits growth [*Mitchell and Holmhansen*, 1991; *Montes-Hugo et al.*, 2009; *Venables et al.*, 2013]. Increased vertical mixing is not likely to have an adverse effect on iron availability in surface waters, due to the abundant supply of shelf sediment-derived iron from UCDW [*Annett et al.*, 2015]. Our data show that the causal relationship between winter sea ice cover and summer chlorophyll, via upper ocean stratification and its control of light availability [*Venables et al.*, 2013], translates robustly to ice-induced changes in nutrient utilisation. As reduced sea ice leads to a reduction in chlorophyll production and nutrient utilisation, we would expect a concomitant reduction in biological CO_2 uptake, such that sea ice dynamics regulate the summer carbon sink.

Table 1. Seasonal average $\delta^{15}N_{NO3}$ for each year and statistical difference data for Welch two-sample t-tests between time-series $\delta^{15}N_{NO3}$ data for 2008/09 and each other season

	Seasonal average $\delta^{15}N_{NO3}$ (‰)	t-test p values for each season vs. 2008/09
2004/05	6.9	6.82×10^{-4}
2005/06	7.9	2.55×10^{-6}
2006/07	8.4	4.21×10^{-4}
2008/09	5.3	-
2009/10	7.4	4.39×10^{-13}

Whilst our observations cannot be assumed *a priori* to be representative of the wider WAP region, the physical mechanisms regulating summer chlorophyll levels are consistent between Ryder Bay [*Venables et al.*, 2013] and further north near Palmer Station on Anvers Island [*Saba et al.*, 2014]. This suggests that a number of similar processes are at work at least amongst different coastal regions, such that our results from Ryder Bay have some level of relevance further afield along the WAP coast. This is reinforced by the fact that the dominant forcings include coupled climate modes such as the Southern Annular Mode (SAM), which is inherently regional in nature [*Saba et al.*, 2014]. Whilst the magnitude of changes in water column stability and chlorophyll levels inevitably shows considerable spatial heterogeneity throughout the region [*Vernet et al.*, 2008], such that results from a coastal location cannot be scaled-up directly, the regionalised nature of the physical driving mechanisms suggests that our observations from Ryder Bay are likely to have broader relevance at the WAP. Indeed, conditions of low sea ice in winter and low water column stability and chlorophyll levels in summer were also observed at the regional WAP scale between 2007 and 2009 [*Ducklow et al.*, 2012; *Saba et al.*, 2014]. Our results from Ryder Bay suggest that these low chlorophyll conditions may translate to a reduction in nutrient utilisation and potentially carbon uptake over a larger scale than observed directly in this study. Ocean gliders have been used to show that Ryder Bay is broadly representative of the larger Marguerite Bay in terms of its physical structure, properties and the changes therein, which suggests strongly that the dominant physical processes are the same and their magnitudes are broadly equivalent in Ryder and Marguerite Bays [*Venables and Meredith*, 2014]. Whilst there are slight differences in temperature and salinity below ~300 m resulting from a 350 m deep sill at the mouth of Ryder Bay [*Venables and Meredith*, 2014], the similarity between bays above this depth is

most important for nutrient supply from nutrient-rich waters above the sill depth (100 – 300 m; Fig. 3), and the uptake and remineralisation processes observed in the upper ~100 m. The negligible change in nutrient concentrations and $\delta^{15}N_{NO3}$ between 200 and 500 m in Ryder Bay, and the similarity in structure between profiles taken on the same day in Marguerite and Ryder Bays (Fig. 3), further suggests that the sill does not prevent overflow of the deep nutrient source into Ryder Bay, and that the processes regulating nutrient supply, uptake and recycling are consistent between the two bays. As such, we argue that the mechanisms we identify in Ryder Bay are likely to be applicable also to Marguerite Bay, and may have implications at the WAP scale.

Sea ice cover showed a decreasing trend in the WAP region during the last three decades [*Massom and Stammerjohn*, 2010; *Stammerjohn et al.*, 2012]. These sea ice declines are thought to have been driven, at least in part, by a trend towards the positive state of the SAM and resultant increase in the strength and persistence of northerly winds at the WAP, which advect ice southwards [*Holland and Kwok*, 2012; *Marshall et al.*, 2004; *Stammerjohn et al.*, 2008; *Thompson and Solomon*, 2002]. The future climate of the specific WAP region is difficult to predict; however, climate models suggest further greenhouse gas-driven warming around Antarctica more generally during the course of this century [*Stocker et al.*, 2013], and a continuation of the trend towards more positive SAM such that polar westerlies will continue to strengthen and shift polewards [*Meijers*, 2014]. Under such circumstances where these trends drive reductions in sea ice cover in productive coastal regions, the results presented here suggest that nutrient utilisation may be concurrently reduced. The expected parity between nutrient utilisation and biological CO_2 uptake, and the disproportionate role for these coastal regions in regional phytoplankton production and carbon uptake [*Pedulli et al.*, 2014], then raise the possibility that climate-driven sea ice reductions may reduce the ability of the WAP surface ocean to sequester atmospheric CO_2.

If the recent shift towards weaker upper ocean stratification and deeper mixed layers [*Venables et al.*, 2013] continues, results from this study suggest that nutrient dynamics and isotope systematics may be affected beyond the consequences for primary production and nutrient uptake. If primary production is reduced, nitrification is also likely to be reduced concurrently because there would be less organic matter to be remineralised and less ammonium substrate for nitrification. Whether this counteracts the increase in mixed layer nitrification rates that may be favoured by deeper mixed layers [*Fripiat et al.*, 2015b] and the possible increase in entrainment of nitrified nitrate from the base of the euphotic layer into

the upper mixed layer will depend on the extent to which primary production and organic matter availability are reduced.

Changes in the isotope effect of nitrate uptake may also arise from ongoing changes in upper ocean mixing. Whilst the effect of MLD, via light, on the organism-level ε [*DiFiore et al.*, 2010] is not expressed in $\delta^{15}N_{NO3}$ data during this study, this does not preclude an effect, which may become more important in the context of ongoing climatic changes in MLD. We speculate that deeper mixed layers may cause phytoplankton growing in a more variable light regime to fractionate the nitrogen isotopes to a greater extent than in shallower mixed layers with more stable light environments. Deeper mixed layers have also been shown to favour the prymnesiophyte *Phaeocystis antarctica* over diatoms in the polar Southern Ocean [*Alderkamp et al.*, 2012; *Arrigo et al.*, 1999], whilst increased glacial meltwater inputs, which can be expected to continue in response to ongoing glacial retreat throughout the WAP region [*Cook et al.*, 2016], have been shown to favour cryptophytes [*Moline et al.*, 2004]. As such, potential shifts in phytoplankton species composition associated with changes in the physical environment [*Moline et al.*, 2004; *Montes-Hugo et al.*, 2009; *Rozema et al.*, 2016; *Saba et al.*, 2014] could also alter the net community isotope effect, compounding or counteracting the effect of changes in light availability. Whilst variability in the supply of deep-sourced nitrate to the upper ocean with mixed layer depth cannot be assessed with the current dataset, deeper mixed layers are likely to increase supply and the supply/uptake ratio, particularly given the hypothesised reduction in primary production and nutrient uptake. However, increased nutrient supply would be unlikely to be important in terms of primary production and biological carbon uptake overall, because the stability of the upper ocean, and its control on the variability of light levels to which phytoplankton are exposed, is the key factor controlling the magnitude of phytoplankton blooms in the coastal WAP [*Saba et al.*, 2014; *Venables et al.*, 2013]. Nitrogen limitation is rare and short-lived, such that macronutrient availability is not an important control on primary production overall. As such, we hypothesise that any increase in nutrient supply driven by enhanced mixing would not be capable of counteracting the negative effect of a more variable mixed layer light environment on phytoplankton productivity in this setting.

5. Conclusions

A suite of biogeochemical and isotopic approaches is used to improve our understanding of macronutrient supply, uptake and cycling in the WAP coastal ocean, and give unique insight into the nutrient biogeochemistry underlying high primary productivity and a large and productive food web in this region. Full-depth profiles of nitrate concentration are used to calculate a net seasonal nitrate drawdown in Ryder Bay for summer 2009/10 of 1.83 mol N m^{-2} yr^{-1}. Using Redfield stoichiometry, this amounts to a net seasonal carbon uptake by phytoplankton of 12.1 mol C m^{-2} yr^{-1} or 146 g C m^{-2} yr^{-1}, which is comparable to other estimates for the WAP coastal environment. High primary production in the stratified upper ocean is fuelled primarily by macronutrients supplied from underlying source waters and micronutrients from shelf sediments and glaciers. Production is primarily nitrate-based and excess silicic acid from depth promotes a diatom-dominated phytoplankton community overall. The phytoplankton community was more mixed consisting of diatoms and non-diatom species in summer 2009/10, as shown by a $[DIN]/[PO_4^{3-}]$ uptake ratio close to the Redfield ratio and a $[Si(OH)_4^-]/[DIN]$ uptake ratio less than 1. A particularly low $[Si(OH)_4^-]/[DIN]$ uptake ratio at the surface provides evidence for the remineralisation of organic matter occurring at a faster rate than biogenic silica dissolution in the uppermost surface ocean. The mixed assemblage caused a strong drawdown of nutrients in the uppermost surface ocean, which highlights the potential of phytoplankton blooms in Ryder Bay to drive short-lived nitrogen limitation before nitrate and/or ammonium are regenerated in situ or resupplied from deeper waters or by lateral advection. We observe pronounced interannual variability in nutrient utilisation, which matches annual changes in chlorophyll levels driven by winter sea ice duration and upper ocean stratification [*Venables et al.*, 2013]. Low winter sea ice and greater mixing lead to much-reduced stratification and nutrient utilisation the following summer, compared to winters with longer-lived fast-ice cover, such that nutrient utilisation is sensitive to climatic changes. With the expected relationship between nutrient utilisation and biological CO_2 uptake, sea ice changes in the WAP region could hold important consequences for the summer carbon sink, at least in the productive coastal regions, and potentially feedbacks in the ocean-carbon-climate system.

Nitrogen isotopes in nitrate show a utilisation signal from subsurface nutrient source waters to the surface and over the growing seasons. However, our data consistently fall below the expected relationship between $\delta^{15}N_{NO3}$ and nitrate concentration from utilisation alone, suggesting that other processes are at work that lower $\delta^{15}N_{NO3}$ or nitrate concentration or both. The deviation of our data from the Rayleigh closed system utilisation model cannot be

accounted for by resupply of unutilised nitrate from depth or changes in organism-level isotope effect. We show that dilution of surface water nitrate by glacial and sea-ice meltwater plays an important role in modifying the $\delta^{15}N/[NO_3^-]$ relationship, but has a small effect on surface nitrate concentrations compared to utilisation. From a subset of our data, corrected for these dilution effects, we estimate that the community-level isotope effect of nitrate uptake is 4.19 ± 0.29 ‰, in agreement with previous estimates for the polar Antarctic zone. However, the majority of our corrected data still fall below seasonal and modelled utilisation trends. We argue that nitrification at the base of the euphotic layer, either just below or within the deeper part of the mixed layer, during summer is the process most likely to be driving the lowering of upper ocean $\delta^{15}N_{NO3}$ that we observe. Water column nitrification in the deep and poorly-lit winter mixed layer is likely, but is found to have a limited effect on $\delta^{15}N_{NO3}$ values at the beginning of the summer growing season. We suggest that nitrification is also likely to be occurring in sea ice during the winter, although this does not have an appreciable effect on the isotope composition of surface water nitrate, due to the small input of sea-ice nitrate compared to the deep nutrient-rich ocean below. The impact of low-$\delta^{15}N$ nitrified nitrate on the surface ocean nitrate pool is most pronounced when ambient nitrate concentrations are lowest, due to utilisation over the summer phytoplankton blooms.

We propose that the documented control of upper ocean mixing by winter sea ice duration may have important implications for nutrient dynamics and isotope systematics in the WAP coastal ocean, in addition to those for primary production and nutrient utilisation. Ongoing changes in sea ice and coupled upper ocean processes at the WAP may drive changes in water column nitrification and its influence on the surface nitrate pool, in isotopic fractionation by phytoplankton during nitrate uptake, and in the supply of nitrate from depth. Future work will examine the changes in nutrient supply, utilisation and recycling in the water column and sea ice in Ryder Bay and throughout the wider WAP region in response to ongoing changes in the physical environment.

References

Alderkamp, A. C., M. M. Mills, G. L. van Dijken, P. Laan, C. E. Thuroczy, L. J. A. Gerringa, H. J. W. de Baar, C. D. Payne, R. J. W. Visser, A. G. J. Buma, and K. R. Arrigo (2012), Iron from melting glaciers fuels phytoplankton blooms in the Amundsen Sea (Southern Ocean): Phytoplankton characteristics and productivity, *Deep-Sea Res Pt Ii*, *71-76*, 32-48, DOI 10.1016/j.dsr2.2012.03.005.

Annett, A. L., D. S. Carson, X. Crosta, A. Clarke, and R. S. Ganeshram (2010), Seasonal progression of diatom assemblages in surface waters of Ryder Bay, Antarctica, *Polar Biol*, *33*(1), 13-29, DOI 10.1007/s00300-009-0681-7.

Annett, A. L. (2013), Phytoplankton ecology and biogeochemistry of the warming Antarctic sea-ice zone, PhD thesis, 314 pp, University of Edinburgh, Edinburgh, U.K.

Annett, A. L., M. Skiba, S. F. Henley, H. J. Venables, M. P. Meredith, P. J. Statham, and R. S. Ganeshram (2015), Comparative roles of upwelling and glacial iron sources in Ryder Bay, coastal western Antarctic Peninsula, *Mar Chem*, *176*, 21-33, DOI 10.1016/j.marchem.2015.06.017.

Arrigo, K. R., D. H. Robinson, D. L. Worthen, R. B. Dunbar, G. R. DiTullio, M. VanWoert, and M. P. Lizotte (1999), Phytoplankton community structure and the drawdown of nutrients and CO2 in the Southern Ocean, *Science*, *283*(5400), 365-367, DOI 10.1126/science.283.5400.365.

Arrigo, K. R. (2005), Marine microorganisms and global nutrient cycles, *Nature*, *437*(7057), 349-355, Doi 10.1038/Nature04158.

Arrigo, K. R., G. L. van Dijken, and S. Bushinsky (2008a), Primary production in the Southern Ocean, 1997-2006, *J Geophys Res-Oceans*, *113*(C8), DOI 10.1029/2007jc004551.

Arrigo, K. R., G. van Dijken, and M. Long (2008b), Coastal Southern Ocean: A strong anthropogenic CO2 sink, *Geophys Res Lett*, *35*(21), L21602, DOI 10.1029/2008gl035624.

Beardsley, R. C., R. Limeburner, and W. B. Owens (2004), Drifter measurements of surface currents near Marguerite Bay on the western Antarctic Peninsula shelf during austral summer and fall, 2001 and 2002, *Deep-Sea Res Pt Ii*, *51*(17-19), 1947-1964, DOI 10.1016/j.dsr.2004.07.031.

Böhlke, J. K., S. J. Mroczkowski, and T. B. Coplen (2003), Oxygen isotopes in nitrate: new reference materials for 18O:17O:16O measurements and observations on nitrate-water equilibration, *Rapid Commun Mass Sp*, *17*(16), 1835-1846, 10.1002/rcm.1123.

Buesseler, K. O., A. M. P. McDonnell, O. M. E. Schofield, D. K. Steinberg, and H. W. Ducklow (2010), High particle export over the continental shelf of the west Antarctic Peninsula, *Geophys Res Lett*, *37*, DOI 10.1029/2010gl045448.

Caldeira, K., and P. B. Duffy (2000), The role of the Southern Ocean in uptake and storage of anthropogenic carbon dioxide, *Science*, *287*(5453), 620-622, DOI 10.1126/science.287.5453.620.

Carrillo, C. J., R. C. Smith, and D. M. Karl (2004), Processes regulating oxygen and carbon dioxide in surface waters west of the Antarctic Peninsula, *Mar Chem*, *84*(3-4), 161-179, DOI 10.1016/j.marchem.2003.07.004.

Casciotti, K. L., D. M. Sigman, and B. B. Ward (2003), Linking diversity and stable isotope fractionation in ammonia-oxidizing bacteria, *Geomicrobiol J*, *20*(4), 335-353, Doi 10.1080/01490450303895.

Casciotti, K. L. (2009), Inverse kinetic isotope fractionation during bacterial nitrite oxidation, *Geochim Cosmochim Ac*, *73*(7), 2061-2076, 10.1016/j.gca.2008.12.022.

Clarke, A., M. P. Meredith, M. I. Wallace, M. A. Brandon, and D. N. Thomas (2008), Seasonal and interannual variability in temperature, chlorophyll and macronutrients in northern Marguerite Bay, Antarctica, *Deep-Sea Res Pt Ii*, *55*(18-19), 1988-2006, DOI 10.1016/j.dsr2.2008.04.035.

Cook, A. J., P. R. Holland, M. P. Meredith, T. Murray, A. Luckman, and D. G. Vaughan (2016), Ocean forcing of glacier retreat in the western Antarctic Peninsula, *Science*, *353*(6296), 283-286, 10.1126/science.aae0017.

Deutsch, C., and T. Weber (2012), Nutrient Ratios as a Tracer and Driver of Ocean Biogeochemistry, *Annual Review of Marine Science, Vol 4*, *4*, 113-+, DOI 10.1146/annurev-marine-120709-142821.

Dierssen, H. M., R. C. Smith, and M. Vernet (2002), Glacial meltwater dynamics in coastal waters west of the Antarctic peninsula, *P Natl Acad Sci USA*, *99*(4), 1790-1795, DOI 10.1073/pnas.032206999.

DiFiore, P. J., D. M. Sigman, and R. B. Dunbar (2009), Upper ocean nitrogen fluxes in the Polar Antarctic Zone: Constraints from the nitrogen and oxygen isotopes of nitrate, *Geochem Geophy Geosy*, *10*, DOI 10.1029/2009gc002468.

DiFiore, P. J., D. M. Sigman, K. L. Karsh, T. W. Trull, R. B. Dunbar, and R. S. Robinson (2010), Poleward decrease in the isotope effect of nitrate assimilation across the Southern Ocean, *Geophys Res Lett*, *37*, DOI 10.1029/2010gl044090.

Dinniman, M. S., and J. M. Klinck (2004), A model study of circulation and cross-shelf exchange on the west Antarctic Peninsula continental shelf, *Deep-Sea Res Pt Ii*, *51*(17-19), 2003-2022, DOI 10.1016/j.dsr2.2004.07.030.

Dinniman, M. S., J. M. Klinck, and W. O. Smith (2011), A model study of Circumpolar Deep Water on the West Antarctic Peninsula and Ross Sea continental shelves, *Deep-Sea Res Pt Ii*, *58*(13-16), 1508-1523, DOI 10.1016/j.dsr2.2010.11.013.

Dore, J. E., G. Tien, R. Letelier, G. Parrish, J. Szyper, J. Burgett, and D. M. Karl (1992), RACER: Distributions of nitrogenous nutrients near receding pack ice in Marguerite Bay, *Antarctic Journal of the United States*, *27*, 177-179,

Ducklow, H. W., K. Baker, D. G. Martinson, L. B. Quetin, R. M. Ross, R. C. Smith, S. E. Stammerjohn, M. Vernet, and W. Fraser (2007), Marine pelagic ecosystems: The West Antarctic Peninsula, *Philos T R Soc B*, *362*(1477), 67-94, DOI 10.1098/rstb.2006.1955.

Ducklow, H. W., O. Schofield, M. Vernet, S. Stammerjohn, and M. Erickson (2012), Multiscale control of bacterial production by phytoplankton dynamics and sea ice along the western Antarctic Peninsula: A regional and decadal investigation, *J Marine Syst*, *98-99*, 26-39, DOI 10.1016/j.jmarsys.2012.03.003.

Ducklow, H. W., W. R. Fraser, M. P. Meredith, S. E. Stammerjohn, S. C. Doney, D. G. Martinson, S. F. Sailley, O. M. Schofield, D. K. Steinberg, H. J. Venables, and C. D. Amsler (2013), West Antarctic Peninsula: An Ice-Dependent Coastal Marine Ecosystem in Transition, *Oceanography*, *26*(3), 190-203, DOI 10.5670/oceanog.2013.62.

Dugdale, R. C., F. P. Wilkerson, and H. J. Minas (1995), The Role of a Silicate Pump in Driving New Production, *Deep-Sea Res Pt I*, *42*(5), 697-719, Doi 10.1016/0967-0637(95)00015-X.

Fletcher, S. E. M., N. Gruber, A. R. Jacobson, S. C. Doney, S. Dutkiewicz, M. Gerber, M. Follows, F. Joos, K. Lindsay, D. Menemenlis, A. Mouchet, S. A. Muller, and J. L. Sarmiento (2006), Inverse estimates of anthropogenic CO2 uptake, transport, and storage by the ocean, *Global Biogeochem Cy*, *20*(2), DOI 10.1029/2005gb002530.

Franck, V. M., M. A. Brzezinski, K. H. Coale, and D. M. Nelson (2000), Iron and silicic acid concentrations regulate Si uptake north and south of the Polar Frontal Zone in the Pacific Sector of the Southern Ocean, *Deep-Sea Res Pt Ii*, *47*(15-16), 3315-3338,

Fripiat, F., D. M. Sigman, S. E. Fawcett, P. A. Rafter, M. A. Weigand, and J. L. Tison (2014), New insights into sea ice nitrogen biogeochemical dynamics from the nitrogen isotopes, *Global Biogeochem Cy*, *28*(2), 115-130, Doi 10.1002/2013gb004729.

Fripiat, F., D. M. Sigman, G. Masse, and J. L. Tison (2015a), High turnover rates indicated by changes in the fixed N forms and their stable isotopes in Antarctic landfast sea ice, *J Geophys Res-Oceans*, *120*(4), 3079-3097, 10.1002/2014jc010583.

Fripiat, F., M. Elskens, T. W. Trull, S. Blain, A. J. Cavagna, C. Fernandez, D. Fonseca-Batista, F. Planchon, P. Raimbault, A. Roukaerts, and F. Dehairs (2015b), Significant mixed layer nitrification in a natural iron-fertilized bloom of the Southern Ocean, *Global Biogeochem Cy*, *29*(11), 1929-1943, 10.1002/2014gb005051.

Garibotti, I. A., M. Vernet, M. E. Ferrario, R. C. Smith, R. M. Ross, and L. B. Quetin (2003), Phytoplankton spatial distribution patterns along the western Antarctic Peninsula (Southern Ocean), *Mar Ecol Prog Ser*, *261*, 21-39, DOI 10.3354/meps261021.

Gerringa, L. J. A., A. C. Alderkamp, P. Laan, C. E. Thuroczy, H. J. W. De Baar, M. M. Mills, G. L. van Dijken, H. van Haren, and K. R. Arrigo (2012), Iron from melting glaciers fuels the phytoplankton blooms in Amundsen Sea (Southern Ocean): Iron biogeochemistry, *Deep-Sea Res Pt Ii*, *71-76*, 16-31, DOI 10.1016/j.dsr2.2012.03.007.

Granger, J., D. M. Sigman, M. F. Lehmann, and P. D. Tortell (2008), Nitrogen and oxygen isotope fractionation during dissimilatory nitrate reduction by denitrifying bacteria, *Limnol Oceanogr*, *53*(6), 2533-2545, DOI 10.4319/lo.2008.53.6.2533.

Gruber, N., and J. L. Sarmiento (1997), Global patterns of marine nitrogen fixation and denitrification, *Global Biogeochem Cy*, *11*(2), 235-266, Doi 10.1029/97gb00077.

Gruber, N., M. Gloor, S. E. M. Fletcher, S. C. Doney, S. Dutkiewicz, M. J. Follows, M. Gerber, A. R. Jacobson, F. Joos, K. Lindsay, D. Menemenlis, A. Mouchet, S. A. Muller, J. L. Sarmiento, and T. Takahashi (2009), Oceanic sources, sinks, and transport of atmospheric CO2, *Global Biogeochem Cy*, *23*, DOI 10.1029/2008gb003349.

Hofmann, E. E., J. M. Klinck, C. M. Lascara, and D. A. Smith (1996), Water mass distribution and circulation west of the Antarctic Peninsula and including Bransfield Strait, in *Foundations for ecological research west of the Antarctic Peninsula*, edited by R. M. Ross, E. E. Hofmann and L. B. Quetin, American Geophysical Union, Washington, D. C.

Hofmann, E. E., and J. M. Klinck (1998), Thermohaline variability of the waters overlying the west Antarctic Peninsula continental shelf, in *Ocean, ice and atmosphere: interactions at the Antarctic continental margin*, edited by S. S. Jacobs and R. F. Weiss, American Geophysical Union, Washington, D. C.

Holland, P. R., and R. Kwok (2012), Wind-driven trends in Antarctic sea-ice drift, *Nat Geosci*, *5*(12), 872-875, DOI 10.1038/Ngeo1627.

Holmes, R. M., A. Aminot, R. Kerouel, B. A. Hooker, and B. J. Peterson (1999), A simple and precise method for measuring ammonium in marine and freshwater ecosystems, *Can J Fish Aquat Sci*, *56*(10), 1801-1808, DOI 10.1139/cjfas-56-10-1801.

Howard, S. L., J. Hyatt, and L. Padman (2004), Mixing in the pycnocline over the western Antarctic Peninsula shelf during Southern Ocean GLOBEC, *Deep-Sea Res Pt Ii*, *51*(17-19), 1965-1979, DOI 10.1016/j.dsr2.2004.08.002.

Hutchins, D. A., and K. W. Bruland (1998), Iron-limited diatom growth and Si : N uptake ratios in a coastal upwelling regime, *Nature*, *393*(6685), 561-564, Doi 10.1038/31203.

Karl, D., A. Michaels, B. Bergman, D. Capone, E. Carpenter, R. Letelier, F. Lipschultz, H. Paerl, D. Sigman, and L. Stal (2002), Dinitrogen fixation in the world's oceans, *Biogeochemistry*, *57*(1), 47-+, Doi 10.1023/A:1015798105851.

Karsh, K. L., T. W. Trull, A. J. Lourey, and D. M. Sigman (2003), Relationship of nitrogen isotope fractionation to phytoplankton size and iron availability during the Southern Ocean Iron RElease Experiment (SOIREE), *Limnol Oceanogr*, *48*(3), 1058-1068,

Klausmeier, C. A., E. Litchman, T. Daufresne, and S. A. Levin (2004), Optimal nitrogen-to-phosphorus stoichiometry of phytoplankton, *Nature*, *429*(6988), 171-174, 10.1038/nature02454.

Klinck, J. M. (1998), Heat and salt changes on the continental shelf west of the Antarctic Peninsula between January 1993 and January 1994, *J Geophys Res-Oceans*, *103*(C4), 7617-7636, DOI 10.1029/98jc00369.

Klinck, J. M., E. E. Hofmann, R. C. Beardsley, B. Salihoglu, and S. Howard (2004), Water-mass properties and circulation on the west Antarctic Peninsula Continental Shelf in Austral Fall and Winter 2001, *Deep-Sea Res Pt Ii*, *51*(17-19), 1925-1946, DOI 10.1016/j.dsr2.2004.08.001.

Legge, O. J., D. C. E. Bakker, M. T. Johnson, M. P. Meredith, H. J. Venables, P. J. Brown, and G. A. Lee (2015), The seasonal cycle of ocean-atmosphere CO2 flux in Ryder Bay, west Antarctic Peninsula, *Geophys Res Lett*, *42*(8), 2934-2942, Doi 10.1002/2015gl063796.

Lenton, A., B. Tilbrook, R. M. Law, D. Bakker, S. C. Doney, N. Gruber, M. Ishii, M. Hoppema, N. S. Lovenduski, R. J. Matear, B. I. McNeil, N. Metzl, S. E. M. Fletcher, P. M. S. Monteiro, C. Rodenbeck, C. Sweeney, and T. Takahashi (2013), Sea-air CO2 fluxes in the Southern Ocean for the period 1990-2009, *Biogeosciences*, *10*(6), 4037-4054, DOI 10.5194/bg-10-4037-2013.

Mariotti, A., J. C. Germon, P. Hubert, P. Kaiser, R. Letolle, A. Tardieux, and P. Tardieux (1981), Experimental-Determination of Nitrogen Kinetic Isotope Fractionation - Some Principles - Illustration for the Denitrification and Nitrification Processes, *Plant Soil*, *62*(3), 413-430, Doi 10.1007/Bf02374138.

Marshall, G. J., P. A. Stott, J. Turner, W. M. Connolley, J. C. King, and T. A. Lachlan-Cope (2004), Causes of exceptional atmospheric circulation changes in the Southern Hemisphere, *Geophys Res Lett*, *31*(14), DOI 10.1029/2004gl019952.

Martinson, D. G., S. E. Stammerjohn, R. A. Iannuzzi, R. C. Smith, and M. Vernet (2008), Western Antarctic Peninsula physical oceanography and spatio-temporal variability, *Deep-Sea Res Pt Ii*, *55*(18-19), 1964-1987, DOI 10.1016/j.dsr2.2008.04.038.

Martinson, D. G. (2012), Antarctic circumpolar current's role in the Antarctic ice system: An overview, *Palaeogeogr Palaeocl*, *335*, 71-74, DOI 10.1016/j.palaeo.2011.04.007.

Martinson, D. G., and D. C. McKee (2012), Transport of warm Upper Circumpolar Deep Water onto the western Antarctic Peninsula continental shelf, *Ocean Sci*, *8*(4), 433-442, DOI 10.5194/os-8-433-2012.

Martiny, A. C., C. T. A. Pham, F. W. Primeau, J. A. Vrugt, J. K. Moore, S. A. Levin, and M. W. Lomas (2013), Strong latitudinal patterns in the elemental ratios of marine plankton and organic matter, *Nat Geosci*, *6*(4), 279-283, DOI 10.1038/Ngeo1757.

Massom, R. A., and S. E. Stammerjohn (2010), Antarctic sea ice change and variability – Physical and ecological implications, *Polar Science*, *4*(2), 149-186, DOI 10.1016/j.polar.2010.05.001.

Meijers, A. J. S. (2014), The Southern Ocean in the Coupled Model Intercomparison Project phase 5, *Philos T R Soc A*, *372*(2019), DOI 10.1098/Rsta.2013.0296.

Meredith, M. P., I. A. Renfrew, A. Clarke, J. C. King, and M. A. Brandon (2004), Impact of the 1997/98 ENSO on upper ocean characteristics in Marguerite Bay, western Antarctic Peninsula, *J Geophys Res-Oceans*, *109*(C9), C09013, DOI 10.1029/2003jc001784.

Meredith, M. P., and J. C. King (2005), Rapid climate change in the ocean west of the Antarctic Peninsula during the second half of the 20th century, *Geophys Res Lett*, *32*(19), DOI 10.1029/2005gl024042.

Meredith, M. P., H. J. Venables, A. Clarke, H. W. Ducklow, M. Erickson, M. J. Leng, J. T. M. Lenaerts, and M. R. van den Broeke (2013), The Freshwater System West of the Antarctic Peninsula: Spatial and Temporal Changes, *J Climate*, *26*(5), 1669-1684, DOI 10.1175/Jcli-D-12-00246.1.

Mitchell, B. G., and O. Holmhansen (1991), Observations and Modeling of the Antarctic Phytoplankton Crop in Relation to Mixing Depth, *Deep-Sea Res*, *38*(8-9), 981-1007, Doi 10.1016/0198-0149(91)90093-U.

Moffat, C., R. C. Beardsley, B. Owens, and N. van Lipzig (2008), A first description of the Antarctic Peninsula Coastal Current, *Deep-Sea Res Pt Ii*, *55*(3-4), 277-293, DOI 10.1016/j.dsr2.2007.10.003.

Moffat, C., B. Owens, and R. C. Beardsley (2009), On the characteristics of Circumpolar Deep Water intrusions to the west Antarctic Peninsula Continental Shelf, *J Geophys Res-Oceans*, *114*, DOI 10.1029/2008jc004955.

Moline, M. A., H. Claustre, T. K. Frazer, O. Schofield, and M. Vernet (2004), Alteration of the food web along the Antarctic Peninsula in response to a regional warming trend, *Global Change Biol*, *10*(12), 1973-1980, DOI 10.1111/j.1365-2486.2004.00825.x.

Montes-Hugo, M., S. C. Doney, H. W. Ducklow, W. Fraser, D. Martinson, S. E. Stammerjohn, and O. Schofield (2009), Recent Changes in Phytoplankton Communities Associated with Rapid Regional Climate Change Along the Western Antarctic Peninsula, *Science*, *323*(5920), 1470-1473, DOI 10.1126/science.1164533.

Montes-Hugo, M., C. Sweeney, S. C. Doney, H. Ducklow, R. Frouin, D. G. Martinson, S. Stammerjohn, and O. Schofield (2010), Seasonal forcing of summer dissolved inorganic carbon and chlorophyll a on the western shelf of the Antarctic Peninsula, *J Geophys Res-Oceans*, *115*, DOI 10.1029/2009jc005267.

Mosby, H. (1934), *The waters of the Atlantic Antarctic Ocean*, 131 pp., Kommisjon hos Jacob Dybwad, Oslo.

Mosseri, J., B. Queguiner, L. Armand, and V. Cornet-Barthaux (2008), Impact of iron on silicon utilization by diatoms in the Southern Ocean: A case study of Si/N cycle decoupling in a naturally iron-enriched area, *Deep-Sea Res Pt Ii*, *55*(5-7), 801-819, DOI 10.1016/j.dsr2.2007.12.003.

Pedulli, M., J. J. Bisagni, H. W. Ducklow, R. Beardsley, and C. Pilskaln (2014), Estimates of potential new production (PNP) for the waters off the western Antarctic Peninsula (WAP) region, *Cont Shelf Res*, *84*, 54-69, DOI 10.1016/j.csr.2014.05.011.

Prezelin, B. B., E. E. Hofmann, C. Mengelt, and J. M. Klinck (2000), The linkage between Upper Circumpolar Deep Water (UCDW) and phytoplankton assemblages on the west Antarctic Peninsula continental shelf, *J Mar Res*, *58*(2), 165-202, DOI 10.1357/002224000321511133.

Prezelin, B. B., E. E. Hofmann, M. Moline, and J. M. Klinck (2004), Physical forcing of phytoplankton community structure and primary production in continental shelf waters of the Western Antarctic Peninsula, *J Mar Res*, *62*(3), 419-460, Doi 10.1357/0022240041446173.

Pritchard, H. D., S. R. M. Ligtenberg, H. A. Fricker, D. G. Vaughan, M. R. van den Broeke, and L. Padman (2012), Antarctic ice-sheet loss driven by basal melting of ice shelves, *Nature*, *484*(7395), 502-505, DOI 10.1038/Nature10968.

Rafter, P. A., P. J. DiFiore, and D. M. Sigman (2013), Coupled nitrate nitrogen and oxygen isotopes and organic matter remineralization in the Southern and Pacific Oceans, *J Geophys Res-Oceans*, *118*(10), 4781-4794, Doi 10.1002/Jgrc.20316.

Rozema, P., H. Venables, W. van de Poll, A. Clarke, M. Meredith, and A. Buma (2016), Interannual variability in phytoplankton biomass and species composition in northern Marguerite Bay (West Antarctic Peninsula) is governed by both winter sea ice cover and summer stratification, *Limnol Oceanogr*, *accepted*,

Ruiz-Halpern, S., M. L. Calleja, J. Dachs, S. Del Vento, M. Pastor, M. Palmer, S. Agusti, and C. M. Duarte (2014), Ocean-atmosphere exchange of organic carbon and CO2 surrounding the Antarctic Peninsula, *Biogeosciences*, *11*(10), 2755-2770, DOI 10.5194/bg-11-2755-2014.

Saba, G. K., W. R. Fraser, V. S. Saba, R. A. Iannuzzi, K. E. Coleman, S. C. Doney, H. W. Ducklow, D. G. Martinson, T. N. Miles, D. L. Patterson-Fraser, S. E. Stammerjohn, D. K. Steinberg, and O. M. Schofield (2014), Winter and spring controls on the summer food web of the coastal West Antarctic Peninsula, *Nat Commun*, *5*, DOI 10.1038/ncomms5318.

Saino, T., and A. Hattori (1980), 15N natural abundance in oceanic suspended particulate matter, *Nature*, *283*(5749), 752-754,

Saino, T., and A. Hattori (1987), Geographical variation of the water column distrubution of suspended particulate organic nitrogen and its 15N natural abundance in the Pacific and its marginal seas, *Deep Sea Research Part A. Oceanographic Research Papers*, *34*(5), 807-827, http://dx.doi.org/10.1016/0198-0149(87)90038-0.

Sarmiento, J. L., and C. LeQuere (1996), Oceanic carbon dioxide uptake in a model of century-scale global warming, *Science*, *274*(5291), 1346-1350, DOI 10.1126/science.274.5291.1346.

Savidge, D. K., and J. A. Amft (2009), Circulation on the West Antarctic Peninsula derived from 6 years of shipboard ADCP transects, *Deep-Sea Res Pt I*, *56*(10), 1633-1655, DOI 10.1016/j.dsr.2009.05.011.

Schmidtko, S., K. J. Heywood, A. F. Thompson, and S. Aoki (2014), Multidecadal warming of Antarctic waters, *Science*, *346*(6214), 1227-1231, 10.1126/science.1256117.

Schofield, O., H. W. Ducklow, D. G. Martinson, M. P. Meredith, M. A. Moline, and W. R. Fraser (2010), How Do Polar Marine Ecosystems Respond to Rapid Climate Change?, *Science*, *328*(5985), 1520-1523, DOI 10.1126/science.1185779.

Serebrennikova, Y. M., and K. A. Fanning (2004), Nutrients in the Southern Ocean GLOBEC region: variations, water circulation, and cycling, *Deep-Sea Res Pt Ii*, *51*(17-19), 1981-2002, DOI 10.1016/j.dsr2.2004.07.023.

Sigman, D. M., M. A. Altabet, D. C. McCorkle, R. Francois, and G. Fischer (1999a), The delta N-15 of nitrate in the Southern Ocean: Consumption of nitrate in surface waters, *Global Biogeochem Cy*, *13*(4), 1149-1166, Doi 10.1029/1999gb900038.

Sigman, D. M., M. A. Altabet, R. Francois, D. C. McCorkle, and J. F. Gaillard (1999b), The isotopic composition of diatom-bound nitrogen in Southern Ocean sediments, *Paleoceanography*, *14*(2), 118-134, Doi 10.1029/1998pa900018.

Sigman, D. M., and E. A. Boyle (2000), Glacial/interglacial variations in atmospheric carbon dioxide, *Nature*, *407*(6806), 859-869, Doi 10.1038/35038000.

Sigman, D. M., M. A. Altabet, D. C. McCorkle, R. Francois, and G. Fischer (2000), The delta N-15 of nitrate in the Southern Ocean: Nitrogen cycling and circulation in the ocean interior, *J Geophys Res-Oceans*, *105*(C8), 19599-19614, Doi 10.1029/2000jc000265.

Sigman, D. M., K. L. Casciotti, M. Andreani, C. Barford, M. Galanter, and J. K. Bohlke (2001), A bacterial method for the nitrogen isotopic analysis of nitrate in seawater and freshwater, *Anal Chem*, *73*(17), 4145-4153, DOI 10.1021/Ac010088e.

Smart, S. M., S. E. Fawcett, S. J. Thomalla, M. A. Weigand, C. J. C. Reason, and D. M. Sigman (2015), Isotopic evidence for nitrification in the Antarctic winter mixed layer, *Global Biogeochem Cy*, *29*(4), 427-445, 10.1002/2014gb005013.

Smith, C. R., D. J. DeMaster, C. Thomas, P. Srsen, L. Grange, V. Evrard, and F. DeLeo (2012), Pelagic-Benthic Coupling, Food Banks, and Climate Change on the West Antarctic Peninsula Shelf, *Oceanography*, *25*(3), 188-201, DOI 10.5670/oceanog.2012.94.

Smith, D. A., E. E. Hofmann, J. M. Klinck, and C. M. Lascara (1999), Hydrography and circulation of the west Antarctic Peninsula continental shelf, *Deep-Sea Res Pt I*, *46*(6), 925-949, DOI 10.1016/S0967-0637(98)00103-4.

Smith, D. A., and J. M. Klinck (2002), Water properties on the west Antarctic Peninsula continental shelf: a model study of effects of surface fluxes and sea ice, *Deep-Sea Res Pt Ii*, *49*(21), 4863-4886, DOI 10.1016/S0967-0645(02)00163-7.

Smith, W. O., and D. M. Nelson (1985), Phytoplankton Bloom Produced by a Receding Ice Edge in the Ross Sea - Spatial Coherence with the Density Field, *Science*, *227*(4683), 163-166, DOI 10.1126/science.227.4683.163.

Smith, W. O., and J. C. Comiso (2008), Influence of sea ice on primary production in the Southern Ocean: A satellite perspective, *J Geophys Res-Oceans*, *113*(C5), DOI 10.1029/2007jc004251.

Stammerjohn, S. E., D. G. Martinson, R. C. Smith, X. Yuan, and D. Rind (2008), Trends in Antarctic annual sea ice retreat and advance and their relation to El Nino-Southern Oscillation and Southern Annular Mode variability, *J Geophys Res-Oceans*, *113*(C3), DOI 10.1029/2007jc004269.

Stammerjohn, S. E., R. Massom, D. Rind, and D. Martinson (2012), Regions of rapid sea ice change: An inter-hemispheric seasonal comparison, *Geophys Res Lett*, *39*(6), L06501, DOI 10.1029/2012GL050874.

Stocker, T. F., D. Qin, G.-K. Plattner, M. Tignor, S. K. Allen, J. Boschung, A. Nauels, Y. Xia, V. Bex, and P. M. Midgley (Eds.) (2013), *Climate Change 2013: The Physical Science Basis. Contribution of Working Group I to the Fifth Assessment Report of the Intergovernmental Panel on Climate Change*, 1535 pp., Cambridge University Press, Cambridge, UK and New York, NY, USA.

Strickland, J. D. H., and T. R. Parsons (1968), A practical handbook of seawater analysis, edited by T. R. Parsons, Fisheries Research Board of Canada, Ottawa.

Takeda, S. (1998), Influence of iron availability on nutrient consumption ratio of diatoms in oceanic waters, *Nature*, *393*(6687), 774-777, Doi 10.1038/31674.

Thompson, D. W. J., and S. Solomon (2002), Interpretation of recent Southern Hemisphere climate change, *Science*, *296*(5569), 895-899, DOI 10.1126/science.1069270.

Tuerena, R. E., R. S. Ganeshram, W. Geibert, A. E. Fallick, J. Dougans, A. Tait, S. F. Henley, and E. M. S. Woodward (2015), Nutrient cycling in the Atlantic basin: The evolution of nitrate isotope signatures in water masses, *Global Biogeochem Cy*, *29*(10), 1830-1844, 10.1002/2015gb005164.

Vaughan, D. G., G. J. Marshall, W. M. Connolley, C. Parkinson, R. Mulvaney, D. A. Hodgson, J. C. King, C. J. Pudsey, and J. Turner (2003), Recent rapid regional climate warming on the Antarctic Peninsula, *Climatic Change*, *60*(3), 243-274, DOI 10.1023/A:1026021217991.

Venables, H. J., A. Clarke, and M. P. Meredith (2013), Wintertime controls on summer stratification and productivity at the western Antarctic Peninsula, *Limnol Oceanogr*, *58*(3), 1035-1047, DOI 10.4319/lo.2013.58.3.1035.

Venables, H. J., and M. P. Meredith (2014), Feedbacks between ice cover, ocean stratification, and heat content in Ryder Bay, western Antarctic Peninsula, *J Geophys Res-Oceans*, *119*(8), 5323-5336, 10.1002/2013jc009669.

Vernet, M., D. Martinson, R. Iannuzzi, S. Stammerjohn, W. Kozlowski, K. Sines, R. Smith, and I. Garibotti (2008), Primary production within the sea-ice zone west of the Antarctic Peninsula: I-Sea ice, summer mixed layer, and irradiance, *Deep-Sea Res Pt Ii*, *55*(18-19), 2068-2085, DOI 10.1016/j.dsr2.2008.05.021.

Vernet, M., W. A. Kozlowski, L. R. Yarmey, A. T. Lowe, R. M. Ross, L. B. Quetin, and C. H. Fritsen (2012), Primary production throughout austral fall, during a time of decreasing daylength in the western Antarctic Peninsula, *Mar Ecol Prog Ser*, *452*, 45-61, DOI 10.3354/meps09704.

Wallace, M. I., M. P. Meredith, M. A. Brandon, T. J. Sherwin, A. Dale, and A. Clarke (2008), On the characteristics of internal tides and coastal upwelling behaviour in Marguerite Bay, west Antarctic Peninsula, *Deep-Sea Res Pt Ii*, *55*(18-19), 2023-2040, DOI 10.1016/j.dsr2.2008.04.033.

Ward, B. B. (2008), Nitrification in Marine Systems, *Nitrogen in the Marine Environment, 2nd Edition*, 199-261, 10.1016/B978-0-12-372522-6.00005-0.

Waser, N. A., K. Yin, Z. Yu, K. Tada, P. J. Harrison, D. H. Turpin, and S. E. Calvert (1998a), Nitrogen isotope fractionation during nitrate, ammonium and urea uptake by marine diatoms and coccolithophores under various conditions of N availability, *Mar Ecol Prog Ser*, *169*, 29-41,

Waser, N. A. D., P. J. Harrison, B. Nielsen, S. E. Calvert, and D. H. Turpin (1998b), Nitrogen isotope fractionation during the uptake and assimilation of nitrate, nitrite, ammonium, and urea by a marine diatom, *Limnol Oceanogr*, *43*(2), 215-224, 10.4319/lo.1998.43.2.0215.

Weber, T. S., and C. Deutsch (2010), Ocean nutrient ratios governed by plankton biogeography, *Nature*, *467*(7315), 550-554, 10.1038/nature09403.

Weston, K., T. D. Jickells, D. S. Carson, A. Clarke, M. P. Meredith, M. A. Brandon, M. I. Wallace, S. J. Ussher, and K. R. Hendry (2013), Primary production export flux in Marguerite Bay (Antarctic Peninsula): Linking upper water-column production to sediment trap flux, *Deep-Sea Res Pt I*, *75*, 52-66, DOI 10.1016/j.dsr.2013.02.001.

Woodward, E. M. S., and A. P. Rees (2001), Nutrient distributions in an anticyclonic eddy in the northeast Atlantic Ocean, with reference to nanomolar ammonium concentrations, *Deep-Sea Res Pt Ii*, *48*(4-5), 775-793, DOI 10.1016/S0967-0645(00)00097-7.

Figure 1. Maps showing a) the position of Marguerite Bay and Ryder Bay adjacent to the WAP, and b) the RaTS sampling station in Ryder Bay.

Figure 2. Time-series data for Ryder Bay, 2004-2010. a) Sea ice cover for the whole bay (■ inside-right y-axis), where a score of 10 depicts full cover; mixed layer depth (— outside-right y-axis), calculated as the depth at which density is 0.05 kg m^{-3} greater than at the surface; the depth at which PAR is 5 % of its surface value (— outside right y-axis); and chlorophyll *a* concentration at 15 m depth, which is representative of variability over the entire mixed layer (●- left-hand y-axis). Data in (a) taken from *Venables et al.* [2013]. b) Salinity (black line and y-axis) and oxygen isotope-derived sea-ice melt percentage (red line and y-axis) at 15 m, from *Meredith et al.* [2013]. Lower panel shows concentration of c) nitrate, d) phosphate, e) silicic acid, f) ammonium, g) nitrite and h) N* at 15 m for 2004-2010, as well as i) $\delta^{15}N_{NO3}$ and j) $\delta^{15}N_{nr}$ for summer seasons only. Green colouring highlights summer growing seasons, defined as the period when chlorophyll is >1 μg L^{-1}.

Figure 3. Depth profile plots of concentration of a) nitrate, b) phosphate and c) silicic acid, d) potential temperature from the CTD, e) $\delta^{15}N_{NO3}$, molar ratios f) DIN to phosphate and g) silicic acid to DIN, and h) salinity measured during summer 2009/10. The upper 30 m is expanded in each plot to show upper ocean structure and its variability. Sampling dates are as per legend; MB denotes the depth profile taken at a central Marguerite Bay site as an offshore comparison to the Ryder Bay site. Profiles coloured blue were taken during the short-lived early season phytoplankton bloom in December; those coloured green were taken during the larger phytoplankton bloom in February. Profiles coloured black were taken during lower productivity times. In d) and h), grey circles show all data from summer 2009/10 to provide context for the profiles corresponding to full-depth water sampling events, whose line styles match those of the nutrient plots as per legend.

Figure 4. Time-series plots of a) potential temperature, b) salinity, c) nitrate concentration (filled circles) and isotopic signature (open circles), and d) phosphate concentration (filled circles) and N* (open circles), measured at 500 m for UCDW (left hand plots) and at 100 m for WW (right hand plots) during summer 2009/10.

Figure 5. Linear regression plots of a) nitrate (x) and DIN (+) concentration vs. phosphate concentration, and b) silicic acid concentration vs. nitrate (x) and DIN (+) for the entire study period, including depth profile data from summer 2009/10. Nutrient uptake ratios derived from the slopes of the regressions are displayed on the plots; statistical data are given in section 3.5.

Figure 6. All data plotted as $\delta^{15}N_{NO3}$ versus the natural logarithm of nitrate concentration. Symbol type depicts growing season, symbol colour depicts salinity. Modelled relationships (Equation 3) using initial values of $[NO_3^-]_{ini}$ = 25.2 μmol L^{-1} and $\delta^{15}N_{NO3\ ini}$ = 5.6 ‰ and isotope effects of 4 ‰ (pale blue dotted line) and 5 ‰ (grey dotted line) are shown for comparison with measured values. ε calculated from measured values is given for each season.

Figure 7. All data plotted as $\delta^{15}N_{NO3}$ versus the natural logarithm of nitrate concentration, a) with nitrate corrected for dilution by low-salinity waters, and b) with nitrate corrected for dilution and $\delta^{15}N_{NO3}$ corrected for nitrite interference. Symbol type depicts growing season, symbol colour depicts salinity. Modelled relationships (Equation 3) using initial values of $[NO_3^-]_{ini} = 25.2$ μmol L^{-1} and $\delta^{15}N_{NO3\ ini} = 5.6$ ‰ and isotope effects of 4 ‰ (pale blue dotted line) and 5 ‰ (grey dotted line) are also shown. ε calculated from corrected values is given in b) for each season.
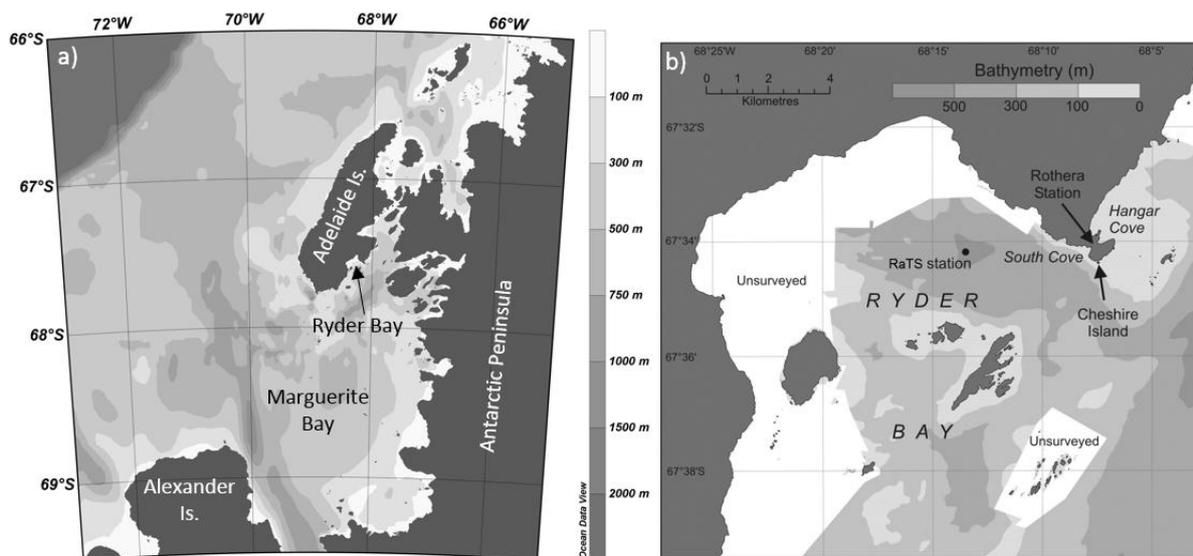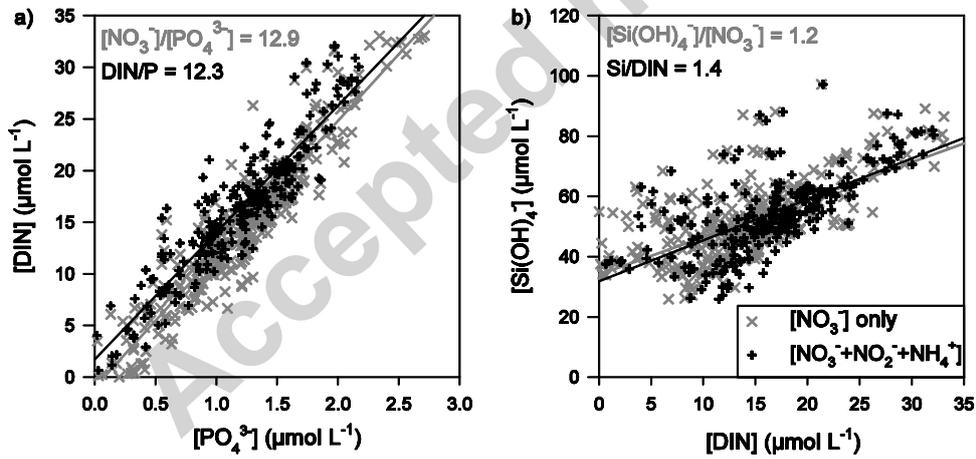

fig. 1
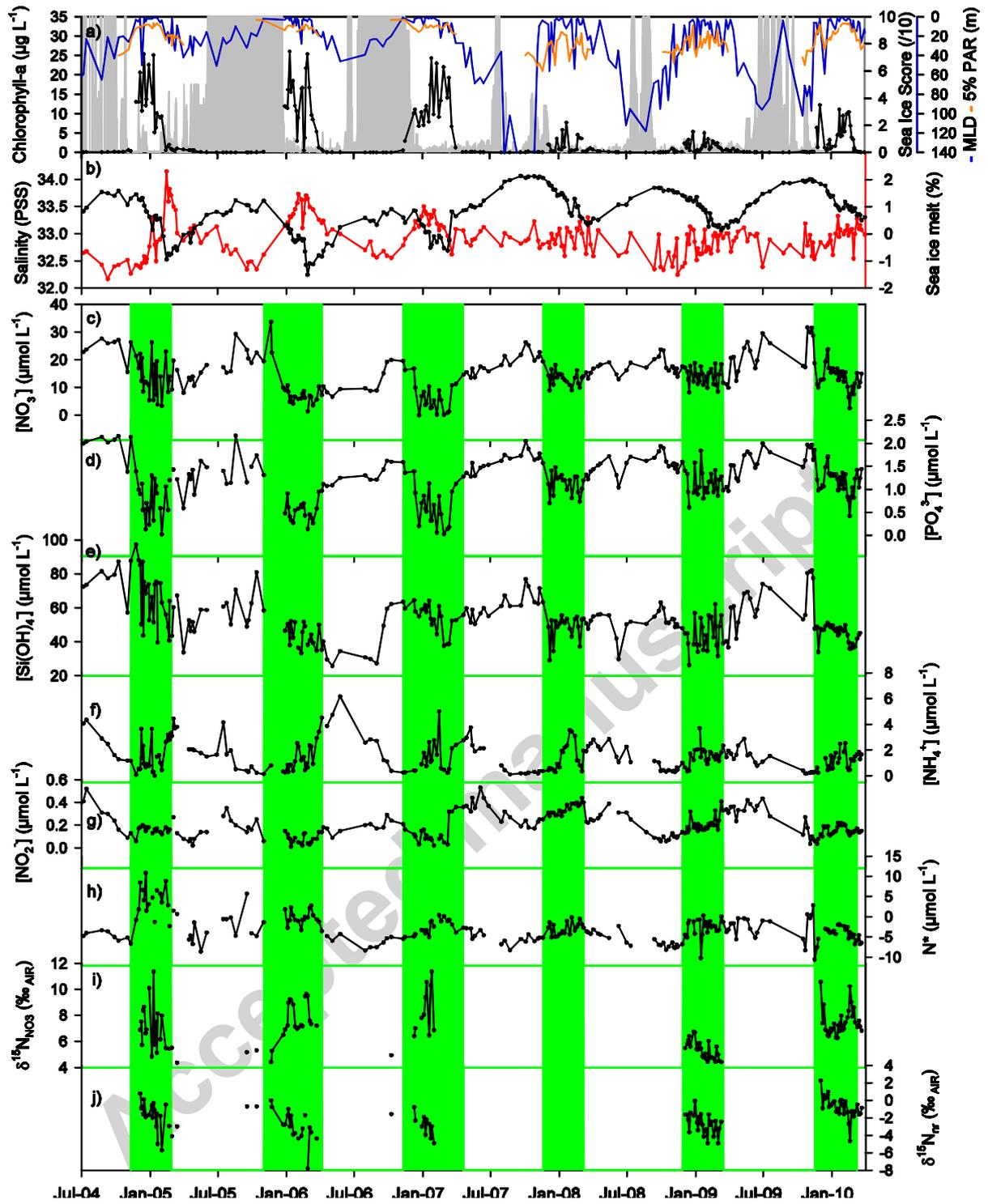
fig. 2
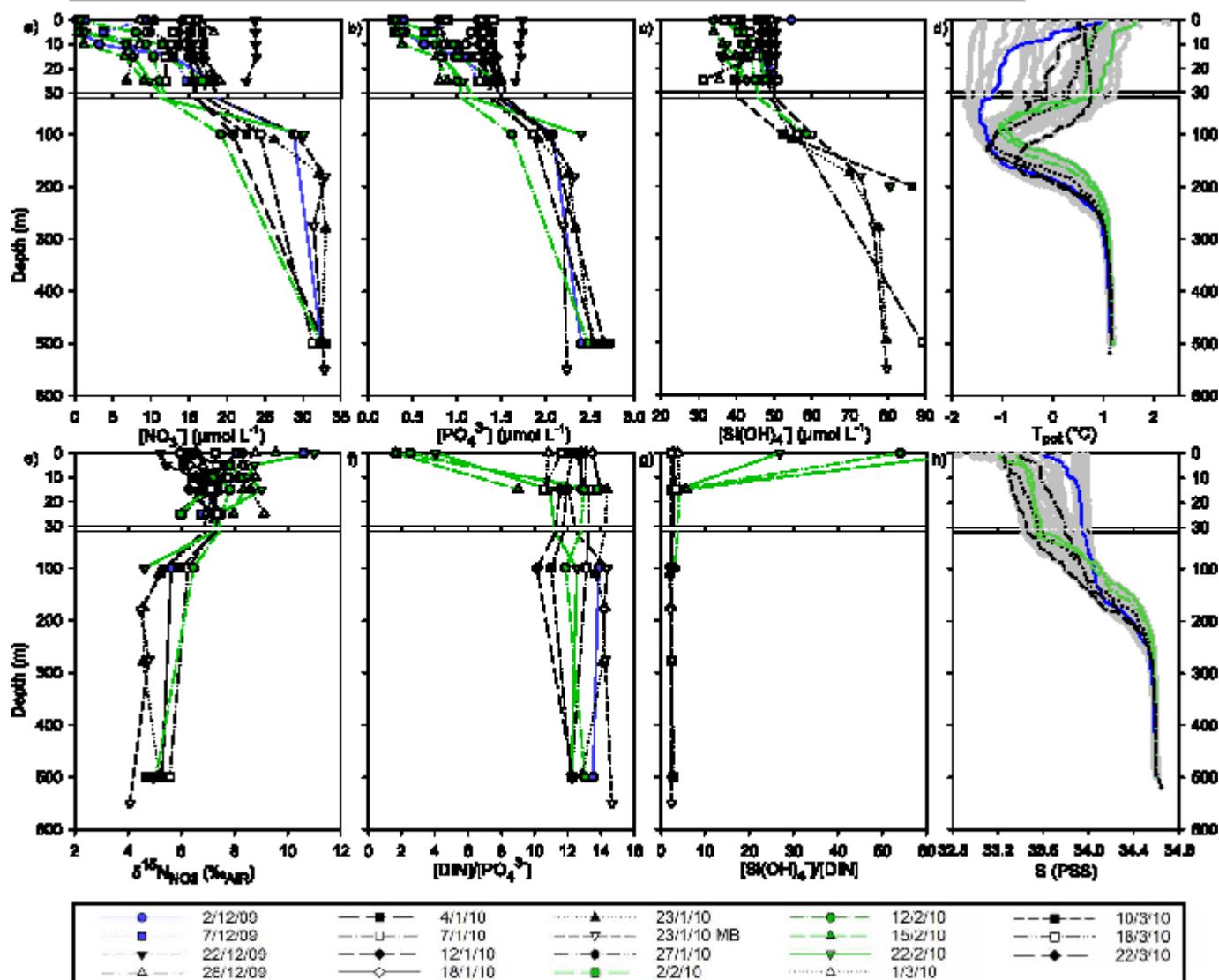
fig. 3
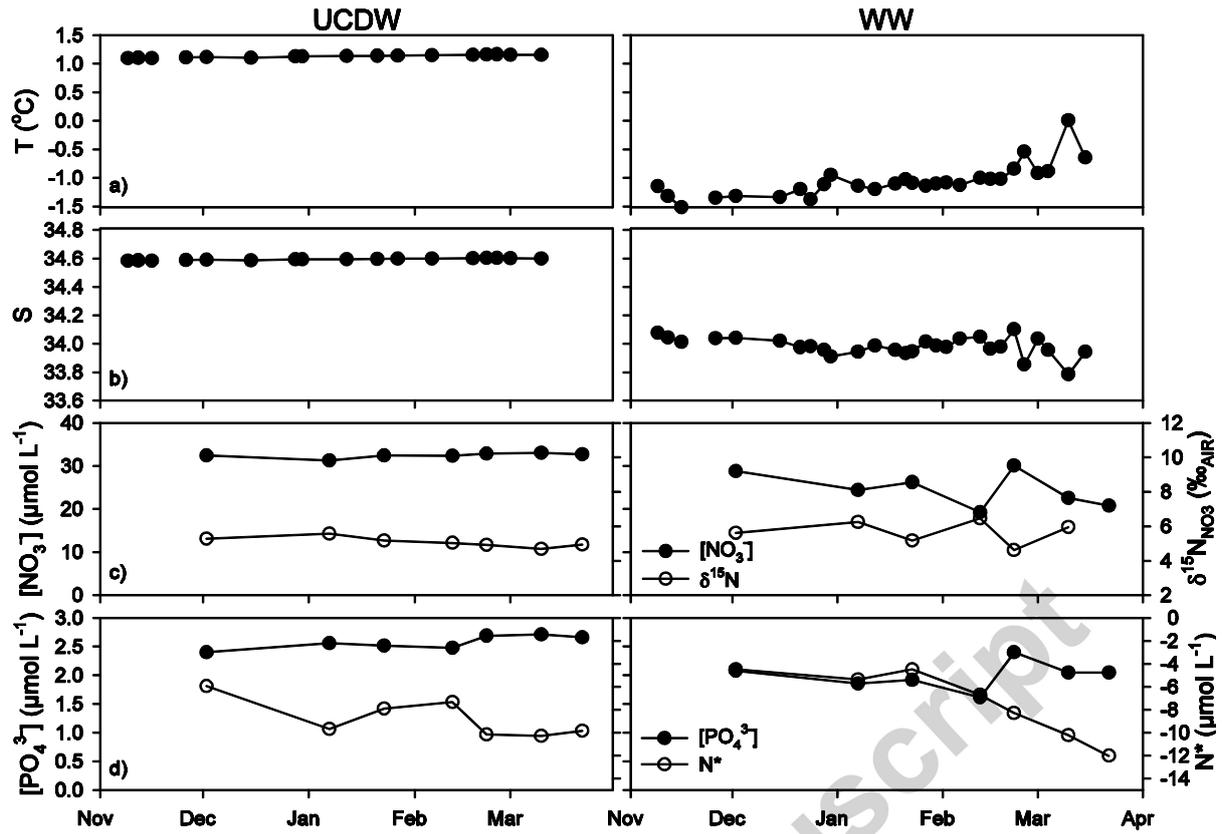
fig. 4

fig. 5

fig. 6

fig. 7a

fig. 7b